

UNCLASSIFIED

AD NUMBER

ADB015022

LIMITATION CHANGES

TO:

Approved for public release; distribution is unlimited.

FROM:

Distribution authorized to U.S. Gov't. agencies only; Administrative/Operational Use; JUN 1976. Other requests shall be referred to Picatinny Arsenal, Dover, NJ.

AUTHORITY

PA ltr 5 May 1977

THIS PAGE IS UNCLASSIFIED

THIS REPORT HAS BEEN DELIMITED
AND CLEARED FOR PUBLIC RELEASE
UNDER DOD DIRECTIVE 5200.20 AND
NO RESTRICTIONS ARE IMPOSED UPON
ITS USE AND DISCLOSURE.

DISTRIBUTION STATEMENT A

APPROVED FOR PUBLIC RELEASE;
DISTRIBUTION UNLIMITED.

FG (2)

ADBOI5022

14

✓ REPORT NO. SARPA-QA-X-019

9 PROGRESS REPORT, Jul 74 - Jul 75,

6 ON BALLISTIC SIMULATORS FOR CHARGE ACCEPTANCE,

10 JOHN K. DOMEN

DDC RECEIVED NOV 16 1976 B

11 JUNE 1976

12 54p.

→ PRODUCTION BASE MODERNIZATION OFFICE
PRODUCT ASURANCE DIRECTORATE
PICATINNY ARSENAL ✓
DOVER, NEW JERSEY 07801

WORK SUPPORTED BY PEMA PROJECTS 5754186 AND 5764302

REPRINT

403982

New
409925



DDC FILE COPY

AD NO.

Report No. QA-X-019

F I S C A L Y E A R 1975

PROGRESS REPORT

on

BALLISTIC SIMULATORS

FOR CHARGE ACCEPTANCE

(Sub-Task of MM&T Project 5754186)

(July 1974 - July 1975)

John K. Domen
June 1976

ACCESSION for	
NTIS	White Section <input type="checkbox"/>
DDC	Buff Section <input checked="" type="checkbox"/>
UNANNOUNCED	<input type="checkbox"/>
JUSTIFICATION.....	
BY.....	
DISTRIBUTION/AVAILABILITY CODES	
Dist.	AVAIL. and/or S. C. 172
B	

Production Base Modernization Office
Product Assurance Directorate
Picatinny Arsenal
Dover, N.J. 07801

The citation in this report of the names of commercial firms or commercially available products or services does not constitute official endorsement or approval of such commercial firms, products, or services by the U.S. Government.

Distribution limited to U.S. Government Agencies only. *T+E*
Other requests for this document must be referred to
Picatinny Arsenal; ATTN: SARPA-QA-X. *16 Nov 76*

TABLE OF CONTENTS

	Page
Introduction	1
List of Illustrations	3
List of Tables	3
A. Dynagun Ballistic Simulator (U. of Illinois)	
A.1 Design Concept	4
A.2 Construction	5
A.3 Firings	9
A.4 Metallic Decelerator	15
A.5 Improvements	23
B. Partial Burner (U. of Massachusetts)	24
C. High Pressure Acoustic Burner (Princeton U.)	32
D. Scalar Gun (Eglin Air Force Base)	43
Conclusions and Recommendations	48
References	49
Distribution List	50

INTRODUCTION

This report summarizes experimental and development work associated with ballistic simulators performed in FY75. Some of the background for this work has already been described (Reference 1) in conjunction with determination of charge loading for propellant charges for the newly designed single and multiple base lines for the Base Modernization Project. Also the present inability of the closed bomb by itself (Reference 2) to adequately determine charge loading for even one zone firing has prompted this work on simulators. The simulator is intended to supplement (not replace) closed bomb tests, by providing extensive and varied dynamic data from propellant thru use of a safe, laboratory device simulating the ballistic gun cycle.

The construction and initial testing at the Univ of Illinois, of the dynagun, (a laboratory simulator for zone 7 of the 155mm howitzer,) has already been reported (references 3, 4). In July 1975, the dynagun with an improved piston, was shipped to Radford AAP for an extensive series of prove-out firings. Due to installation delays, the purchase of more sophisticated data acquisition system and the nonavailability of desired production propellant, initial testing is now planned for Aug 76.

The partial burner experiments have continued at the Univ of Massachusetts and have principally addressed the mode of ignition used in the dynagun. Variations in ignition and early low pressure flame spread phenomena have been investigated.

The scalar gun is a smooth bore 33mm artillery piece at Eglin Air Force Base which fires inert slugs. Simulation of zone 7 of the 155mm Howitzer was done in this device with AUTOCAP M1 propellant, after an initial test series with M6 propellant for the 175mm gun. Although the scalar gun data was limited to a few M1 lots, the results were encouraging. No further testing however is presently planned for the scalar gun, since it was originally intended as a backup for the dynagun simulator which promises to be highly successful.

The high pressure acoustic burner, a compact laboratory burn rate measuring device which burns propellant under liquid at preselected pressure levels up to 50,000 psi, was constructed and tested at Princeton University, and monitors a small pressure increase and ultra high frequency acoustic emission during burn. After initial testing to optimize the ignitor system, further tests on single, multi-base, and solvent rich propellant are planned. The initial intent of

the burner was to obtain unambiguous, direct burn rate measurement at preselected pressure levels for use in interior ballistic computer codes for muzzle velocity prediction. Experimental burn rate is a key input for these codes, which presently, even with closed bomb computed rates, can predict muzzle velocity generally to about 1% (Reference 5). Computer simulation of interior ballistics as an analytical approach for charge determination lies on a plane parallel with ballistic simulators. The unusual data features of the burner have indicated its usefulness as a basic quality control device for propellant in addition to burn rate measurement, and this aspect is currently being investigated.

These experimental tasks were supported by PEMA Projects 5754186 and 5764302.

Background information on the dynagun, the scalar gun, the partial burner, and the high pressure acoustic burner is reported in the 11th JANNAF Combustion Meeting, Vol. 1, Jet Propulsion Laboratory, Pasadena, California, Sept. 1974, pp. 31, 45, 157, and 409. (CPIA Publication No. 261)

List of Illustrations

<u>Figure</u>	<u>Title</u>	<u>Page</u>
1	Mounted Dynagun, Breech End	6
2	Mounted Dynagun, Deceleration End	6
3	Partial Burner	6
4	Detail of Improved Dynagun	7
5	Lot J Howitzer-Dynagun Firing	10
6	Lot K Dynagun Repeatability	11
7	Dynagun Lots P-W Polaroids	16
8	Howitzer and Dynagun Peak Breech Pressure	18
9	Dynagun Lot R Firing	20
10	Invar Tube Inversion Load	22
11	Dynagun Data Acquisition System	24
12	Partial Burner Instrumentation	25
13	Low Pressure, Density Partial Burner Tests	27
14	Closed Bomb Plotting of Burner Tests.....	27
15	Partial Burner--Dynagun Pressure Match	28
16	Closed Bomb Plotting at High Density	28
17	Pressure-time for Ignitor Variation	30
18	Burst Ignitor Uniformity	31
19	Burst Ignitor on AUTOCAP Lots	33
20	Acoustic Burner Pump	34
21	High Pressure Acoustic Burner	35
22	Combustor and Accumulator.....	36
23	Multi-Grain Ignition Core.....	36
24	Acoustic Burner Trace	38
25	Selected Lot U Acoustic Burner Firings	39
26	Burn Rate Plot Comparison	41
27	Eglin Scalar Gun	43
28	Case-Slug Assembly for Scalar Gun	44
29	Scalar Gun-155mm Simulator Plot.....	46
30	Pressure-time for Lot S	47

List of Tables

<u>Table</u>	<u>Title</u>	<u>Page</u>
1	Dynagun-Howitzer Design Parameters	5
2	Dynagun Firings at U. of Illinois	12
3	Howitzer and Dynagun Pressure, Velocity.....	19
4	Acoustic Burner Burn Rates	38
5	Ballistics Calculation for Lot U	40
6	Scalar Gun Parameters for 175mm, 155mm	44
7	Scalar Gun Simulation of 155mm, M126.....	44

A. THE DYNAGUN BALLISTIC SIMULATOR

A.1 Design Concept

Past unreliability of the constant volume closed bomb in arriving by itself at a dependable ballistic assessment has led to the development of a variable volume test device called the "dynagun," termed so in measuring not only pressure but also the dynamic piston motion during volume increase. Modernization of the U.S. Army propellant production has created the need for real time assessment of lot charge weights, and an on-site ballistic evaluation of propellant on a virtually an as-produced basis. The dynagun has the features of a safe, laboratory device with a proving ground capability at the manufacturer's plant.

Two guiding criteria were used in design of the dynagun which is presently scaled for the 155mm, M126 howitzer:

- (1) Equivalent loading density: $L: W_p/V_{CO} = w_p/v_{CO}$
- (2) Newtonian constraint of equivalence of the same fractional chamber volume increase down bore at any time on the assumption that ideally, the pressure-time profiles for both the gun and simulator remain invariant:

$$N: \underbrace{W_s V_{CO} / D_s^4}_{\text{Gun}} = \underbrace{w_s v_{CO} / d_s^4}_{\text{Simulator}}$$

where: W_p - weight of propellant
 W_s - weight of shell or piston
 V_{CO} - initial chamber volume (without propellant)
 D_s - bore diameter

with similar definitions for the simulator, when small letters are used.

The dynagun was designed as a frictionless system and some adjustment in either loading density or slug mass is needed. Presently the massive piston helps compensate for the omission of shot start pressure (none is used and mechanical design complexity was avoided). However, the greater heat loss in the simulator from a large chamber area/volume ratio shows a decreased pressure history from that of the gun. This has been partially compensated not by piston mass change, but by increasing loading density.

The Newtonian constraint is elementary, and with rotation and resistance down bore neglected, is simply:

$$\text{Two integrations of: } \ddot{X} = PA/M_s \qquad \ddot{x} = p a_s / m_s$$

$$\text{Result: } \frac{\Delta V_C}{V_{CO}} = \frac{A_s^2}{M_s V_{CO}} \qquad \text{want } \Rightarrow \frac{\Delta v_c}{v_{CO}} = \frac{a_s^2}{m_s v_{CO}}$$

where P - pressure
 A_s - bore area
 M_s - slug mass
 X - shell travel
 V_C - time dependent volume

From the Newtonian constraint, the ratio of travel (or velocity) in the dynagun to travel in the gun is given by the ratio R and is a measure of the relative decrease in barrel length for the simulator:

$$R = \frac{v_{CO}}{V_{CO}} \left(\frac{D_S}{d_S} \right)^2$$

A.2 Dynagun Construction:

Figures 1, 2 show the dynagun set-up as originally installed at the University of Illinois facility. (Figure 2 shows the deceleration chamber in the foreground). (Figure 3 shows the partial burner at the University of Massachusetts used to study the dynagun ignition system.) Figure 4 sketches the present dynagun which incorporates a redesigned piston with a metal forming die attached to the piston face. An invar tube employing type D inversion serves as the metallic decelerator for the piston. The old design employed a flat piston face and a long cylinder of Hexcel aluminum which presented an average, constant decelerating force of about 39,000 lb.

Pressure accelerates the piston for a distance of 13.3 inches at which time the device begins to vent. After a few more inches of travel, the piston in the original design began engaging the metallic energy absorber of Hexcel corrugated aluminum cylinder measuring about 5x22" for integral piston recovery. (The present configuration with an invar tube has negligible travel from venting to engagement).

The design features of the dynagun and values for zone 7 of the 155mm howitzer M126 are listed in Table 1:

Table 1 Dynagun-Howitzer Design Parameters

	Dynagun	Howitzer(155mm)
Chamber volume v_{CO} (in ³)	8	805 + 15
Slug diameter d_S (in)	1.5	6.1
Slug weight w_S (lb)	35.5	95 (M107)
Propellant weight w_p (lb)	0.132	13.28 (Z7,M4A2)
Travel x_S (in)	13.3	116
Shot start pressure (psi)	0	~4000
Chamber psi at exit	~12,000	~16,000
Slug speed u (fps)	~290	1850
$R = \frac{v_{CO}}{V_{CO}} \left(\frac{D_S}{d_S} \right)^2 = 0.164$		

Approximate performance is illustrated by the use of the ratio R and assuming about 9% friction compensation for the gun or howitzer:

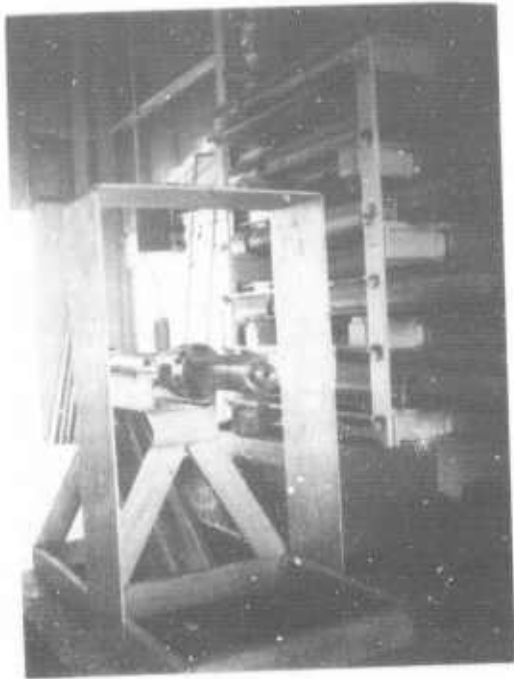


Figure 1. Mounted Dynagun, Breech End

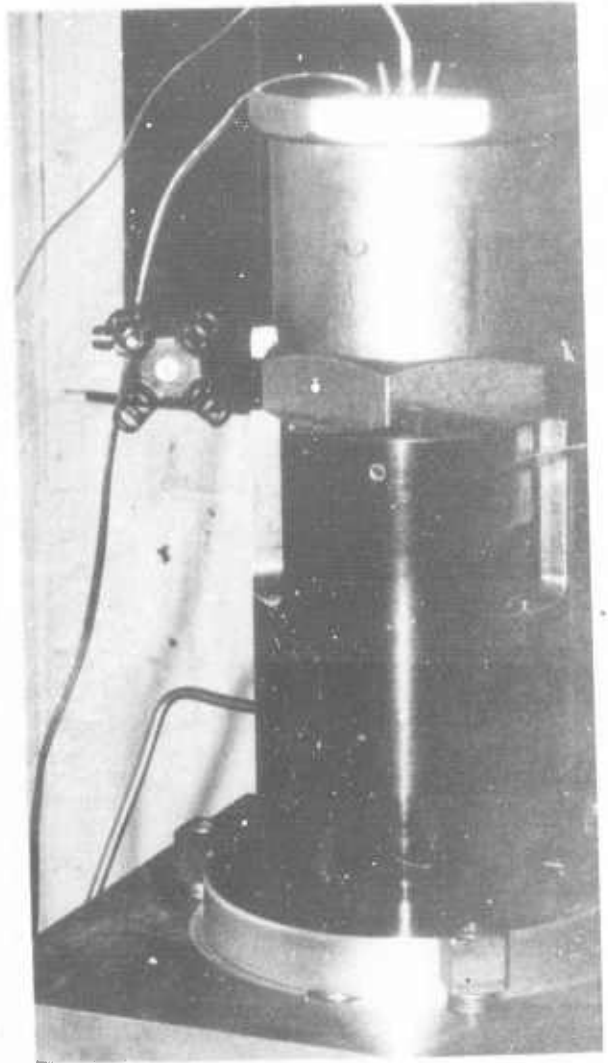


Figure 3. Partial Burner

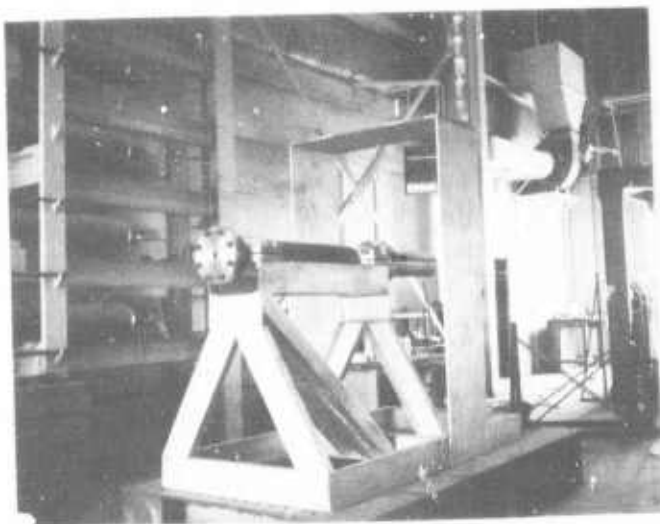


Figure 2. Mounted Dynagun, Decelerator End

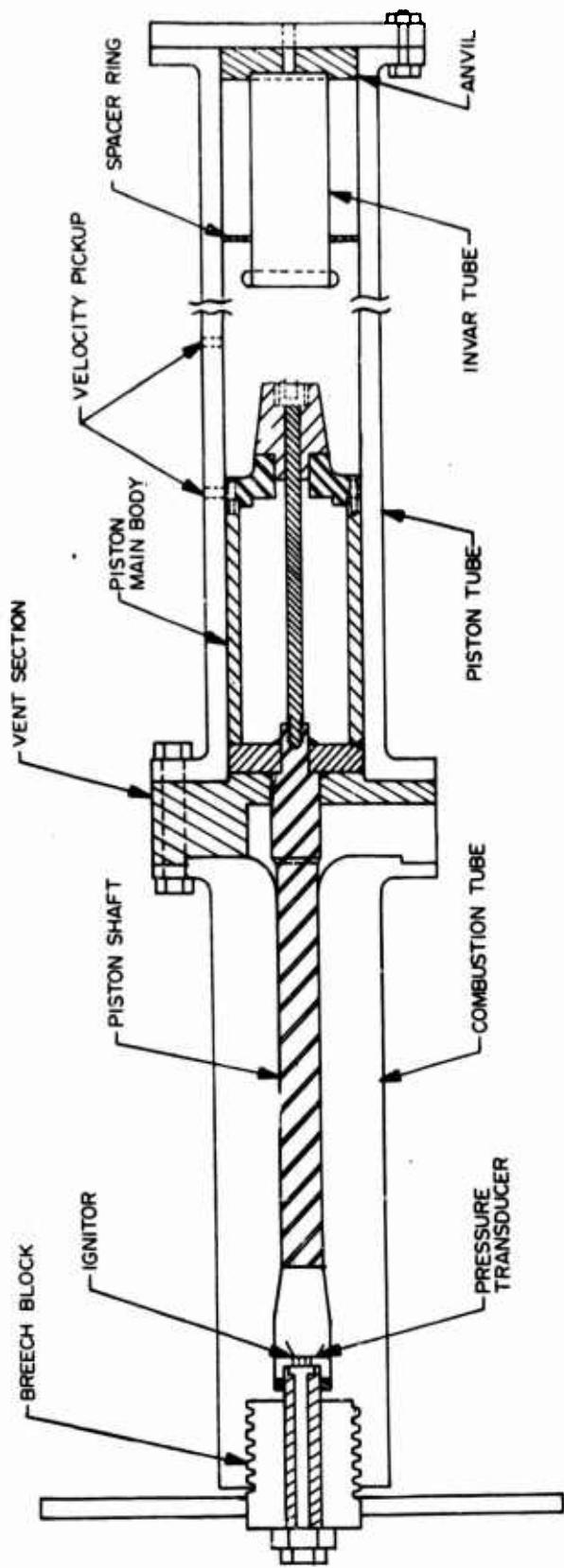


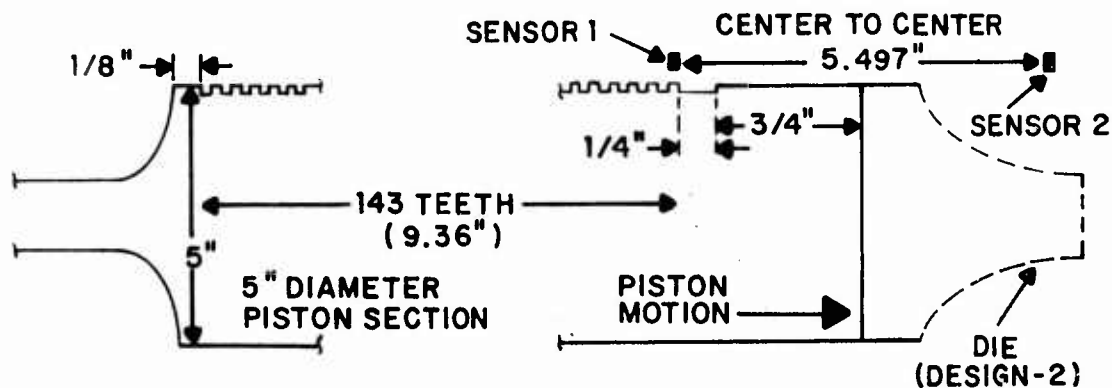
Figure 4. Detail of Improved Dynagun

	Propellant Burn complete	Geometry R = 0.164	Assume gun friction (up by 9%)
X	73 inches	12	13.2
U	Heppner curve 1650 fps	270	290 fps

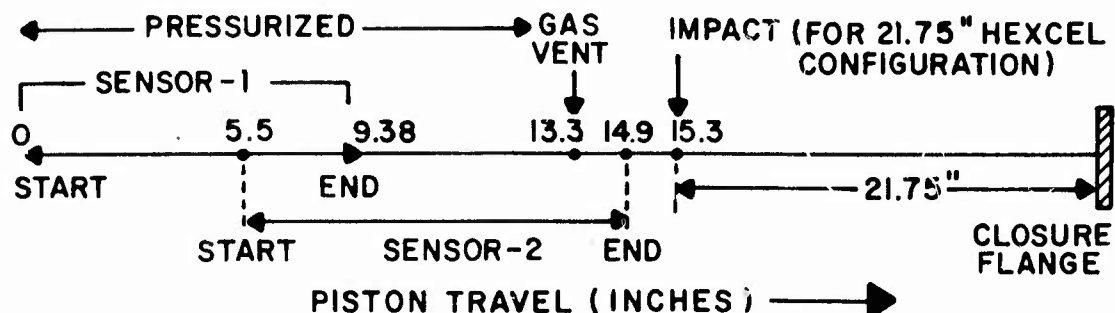
The R ratio indicates in this case that ideally the piston should travel $(116) (0.164) = 19$ inches, were it to move under an identical pressure curve with proportional heat loss.

A lot K firing (typical M4A2 propellant) indicated a piston speed of about 270 fps at 13.2 inch travel.

The dynagun measures six feet long and pressure beyond 40 kpsi has been attained. It exhibits higher heat losses than the 155mm howitzer, which it simulates through the pressure trace. Data is acquired from a breech pressure transducer (Kistler 217C and 587D piezotron coupler), and piston velocity from a F/V converter that monitors a position magnetic pickup sensor mounted in the piston tube wall. A narrow (1/4") steel tooth rack 9.37" long with dimetral pitch of 48 is inlaid in a channel axially down most of the length of the 5" diameter portion of the piston. The rack produces $48/\pi = 15.28$ pulses/inch of travel. The magnetic sensor arrangement employed two sensors: sensor one monitored the entire racklength; sensor two, positioned 5 inches down, and 90 degrees around the tube, merely served as marker for 4 inches of piston motion. (A new arrangement will have sensor two in line with the first, with the same instrumentation as the first). The relative position of sensor and rack are shown:



Events occurring during piston travel of 15.3 inches are:



The final piston speed should be no greater than 300 fps, and for the present design this is comparable to a peak magnetic "square" wave frequency of $(300)(15.28)(12) = 55$ KHz.

The ignitor employs an Atlas match with a 6 volt battery, with the dynagun serving as ground. The battery is shorted for several milliseconds after ignition. Two grams of CBI are tissue wrapped around the match, and the assembly butted against the propellant. (The ignitor alone can account for about 1200 psi pressure contribution).

A.3 Dynagun Firings:

Dynagun firing data was recorded on a polaroid with a four channel trace oscilloscope. Sixty-eight firings of the dynagun have been conducted and a summary is given in Table 2. Observations are:

- a) Black powder was abandoned for CBI for avoid adverse effect on metal finish.
- b) Commercial sliding seals were ineffective above 30 kpsi. Simple nylon machined seals performed better. Type of nylon showed a difference.
- c) The hexcel corrugated aluminum cylinder, 5" x 22" performed excellently in piston deceleration, but was cost prohibitive.

d) The magnetic position sensor failed to operate consistently until the air gap was increased. The influence of larger heat loss in the dynagun is illustrated in Figure 5 where lot J firing is compared for both the simulator and the Aberdeen howitzer. The dynagun charge loading was increased by 11% over zone 7 firing, but the 0.515 g/cm^3 loading still did not achieve peak pressure as attained in the gun. (The slug weight could have been increased, but was not done).

For a repeatability test, four firings were made of lot K (only peak pressure available for one). Figure 6 shows the scatter the dynagun produced. The velocity curves are a result of integrating the pressure curves.

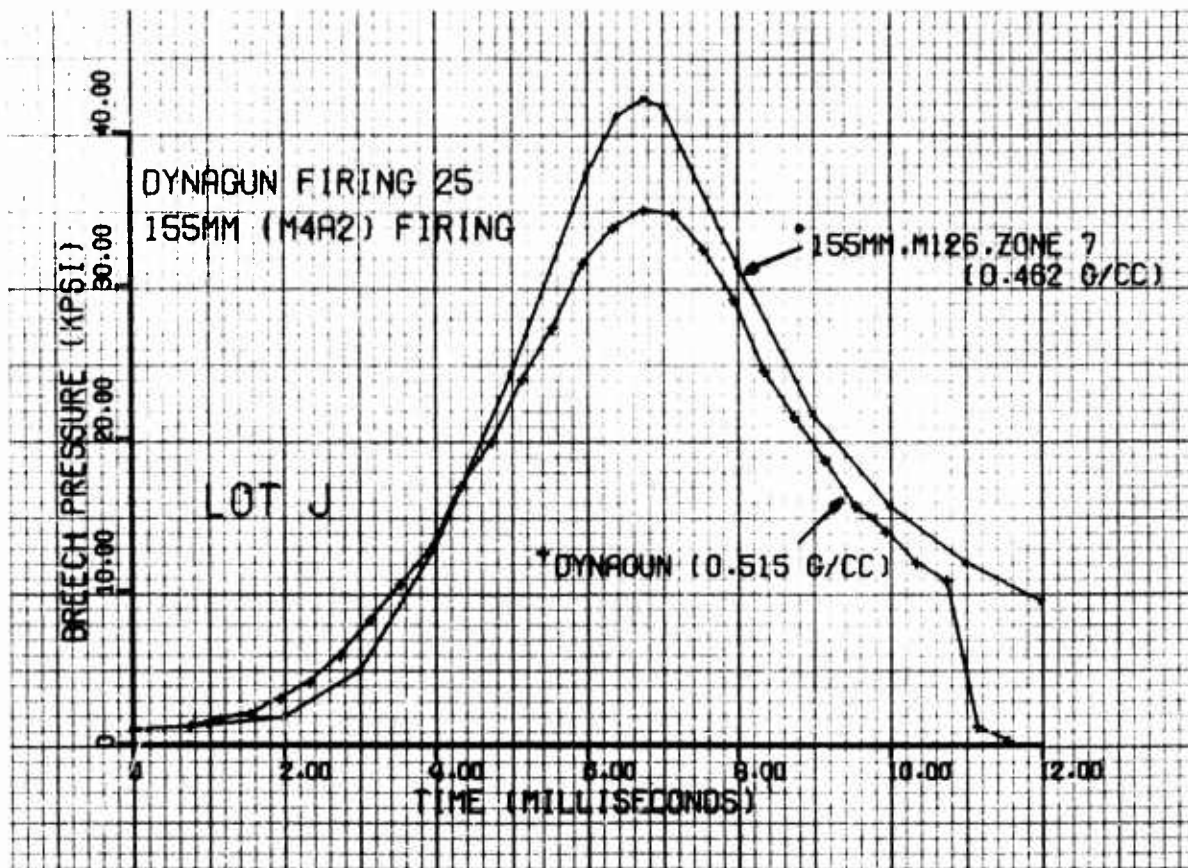


Figure 5. Lot J Gun-Dynagun Firing.

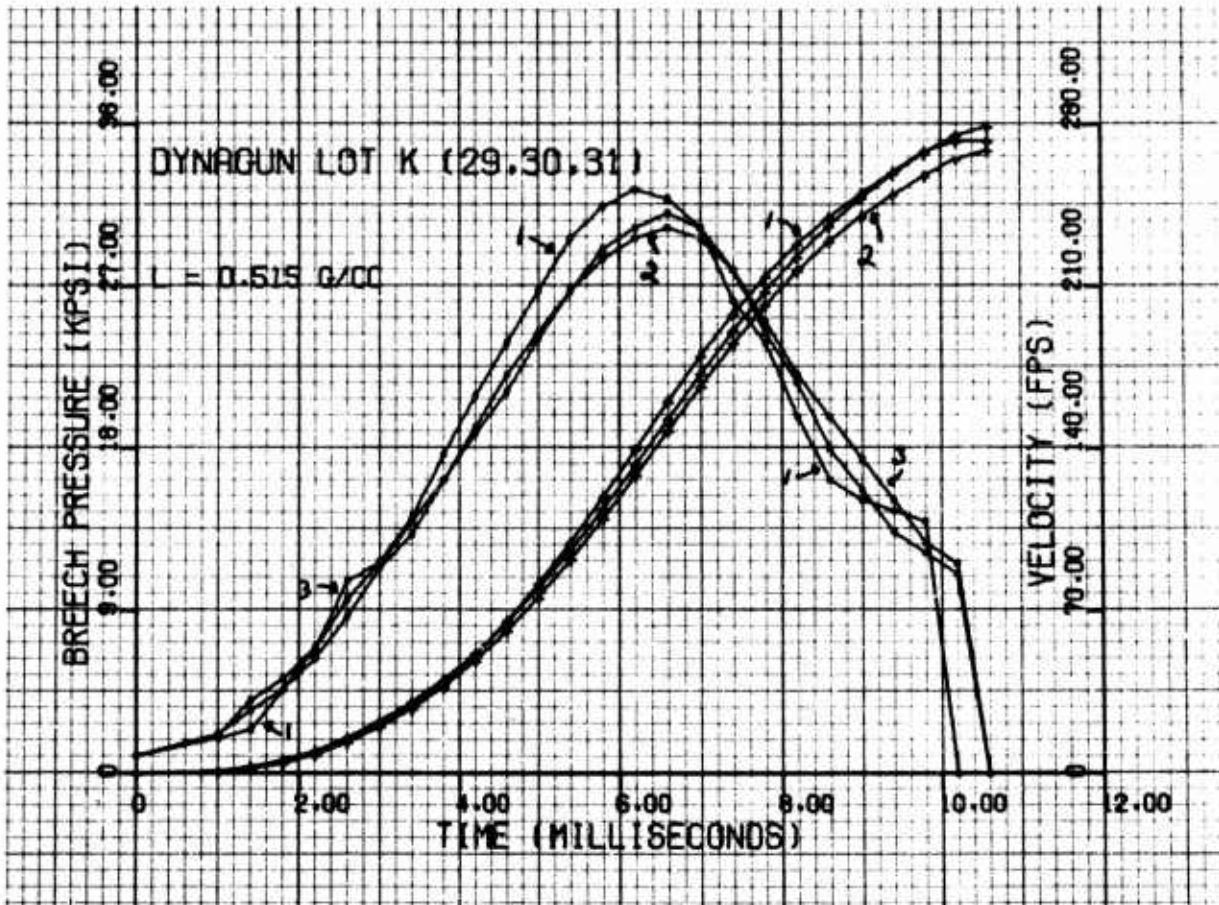


Figure 6. Lot K Dynagun Repeatability.

Table 2 Dynagun Firings at U. of Illinois

Date	#	Seal ^a	Propellant Lot	CWgrams	Energy Abs ^b	Preak Press (kpsi)	Vent Press (kpsi)	Room ^c Tem F	Comments ^d
9/6/74	2	1	K	43.6	3.06	10.8		74	ND,PSF
9/21	3	1	K	43.6	4.50	11.2	7.6	66	
9/21	4	1	K	43.6	4.50	10.8	7.5	66	
9/26	5	1	J	43.6	5.25	13.2	8.1	70	
10/3	6	1	K	59.3	9.25	26.0	10.0	55	
10/10	7	1	K	59.3	9.12	24	10.0	67	PSF
10/15	8	3	K	59.3	9.15	25.6	10.0	62	
10/17	9	3	K	70.0	11.87	43.0	14.0	70	
10/31	10	4	K	64.93	8.81	29.0	12.0	74	PSF
10/31	11	4	J	65.05	11.06	33.5	12.0	74	
11/15	12	4	K	64.88	10.94	33.0	12.0	65	
11/7	13	2	M	65.24	9.75			60	ND
11/12	14	2	K	43.8	4.38			54	TIP
11/16	15	2	K	43.8	4.63			67	GO
11/21	16	2	N	64.98	11.06	32.0	13.0	64	NPG
11/21	17	2	L	65.13	9.75	27.8	13.0	65	
11/23	18	2	M	65.12	9.13	26.0	13.0	67	
11/23	19	2	JL	65.33	9.91	29.0	12.0	67	
12/3	20	2	JKL	65.33	10.75	28.5	12.0	60	
12/5	21	2	K	54.98	7.8	23.0	12.0	66	SUS,PL
12/5	22	2	P	55.17	7.4	18.3	10.0	67	SUS,PL
12/5	23	2	Q	55.11	5.5	16.5	10.5		SUS,PL
12/12	24	2	K	67.47	10.1			66	ND
1/17	25	4	J	67.52		35.5	11.0		
	26	4	K	67.55		30.2			
	27	4	K	43.77		10.			
	28	4	K	67.56		25.	10.		PSF
	29	4	K	67.52		32.4	12.0		
	30	4	K	67.50		30.1	12.0		
	31	4	K	67.50		30.8	14.0		
2/26	32	4	P	67.5	9.22	25.5		44	OGU
3/5	33	5	Q	67.5	9.84	22.5		58	SUS
3/7	34	4	R	67.5	12.47	43.7	16.3	56	PRT
4/2	35	5	S	67.5	11.72	41.2		63	
4/4	36	5	T	67.5	9.72	24.1		46	NS
4/4	37	4	U	67.5	9.34			44	ND
4/5	38	4	U	67.5	8.34	21.2		56	NS
4/5	39	5	V	67.5	11.44	40.0		56	
4/5	40	5	W	67.5	10.53	35.5		56	

Table 2 Dynagun Firings at U. of Illinois (Cont'd)

Date	#	Seal ^a	Propellant Lot	CWgrams	Energy Abs ^b	Preak Press (kpsi)	Vent Press (kpsi)	Comments ^d
4/5/75	41	4	K	22.0	A	5.5		
4/5	42	1	K	22.0	A	6.		
4/5	43	1	K	35.0	A	16.		
	44	5	P	67.5		23.	10.	
	45	5	Q	67.5				ND
	46	5	R	67.5		38.	10.	
	47	5	S	67.5		37.	10.	
	48	5	U	67.5		22.	10.	
	49	5	V	67.5		38.	10.	
	50	5	Q	67.5		19.	11.	
	51	5	T	67.5		20.	10.	
	52	5	W	67.5		25.	12.	
	53	5	K	25.0	A	12.		
	54	5	K	35.0	A	16.		
	55	5	K	35.0	A			
	56	5	K	38.0	A			ND
	57	5	K	15.0	A			
	58	5	K	38.0	A			
	59	5	K	5.0	A			
	60	5	K	38.0	A			
	61	5	K	45.0	A			
	62	5	K	48.0	A			ND
	63	5	K	42.0	B			
	64	5	K	47.8	B			
	65	5	K	48.2	B			
	66	5	K	50.2	B			
	67	5	K	60.1	B			
	68	5	K	70.1	B			

a Seal types: 1-Bal seal; 2-Bal seal with no spring;

3-Nylon seal A; 4-Nylon seal B; 5-Nylon seal C.

b Number represents inches of crushup of Hexcel corrugated aluminum cylinder. A -16 gage SAE 1018 tube.

B -13 gage SAE 1018 tube.

c Propellant charges were temperature preconditioned at 56°F after test 31.

d Notes: No ignitor was used in shots 1 and 2, only few broken grains.

2 grams of black powder was used from shots 3 to 9.

2 grams of CBI was used from shots 10 to 68.

Table 2 (Cont'd)

ND--no data	TIG--trigger from ignitor
NS--nicked seal	pulse; CBI 40 ms delay
PSF--possible seal failure	GO---garbled output
NPG--new pressure gage	OGU--one grain unburned
PRT--propellant reached room temperature	
SUS,PL--some unburned slivers, pressure loss evidence	

All firings from 28 afterward gave D/A converter velocity data after gap adjustment. Firings 16, 17 and 25 gave 258, 242, and 264 fps respectively. Firings 41, 42 and 43 gave 85, 96 and 140 fps during the initial investigation of 16 gage invar tubing.

Afterwards AUTOCAP lots P through W were fired and the original polaroid traces are shown in Figure 7. The traces are: 1) Pressure (high pass filter on amplifier allowed higher frequency through the electronics); 2) the square wave from the digital magnetic sensor (Electro 58405); 3) 4" marker one-shot; 4) velocity from the frequency to voltage converter (Philbrick-Teledyne 4704).

Inasmuch as the pressure signal was the most dependable, Figure 8 shows plotted the peak pressures observed for the various propellants for both the dynagun and 155mm zone 7.

Table 3 compares the maximum pressure and velocity attained in both gun and dynagun using lot K as a reference. The present instrument error in the piston speed is about $\pm 3\%$.

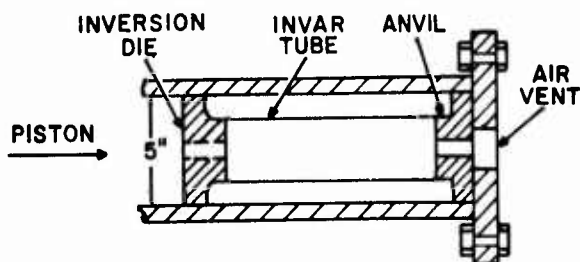
Finally in Figure 9, the pressure for firing 34 (lot R) as well as could be read from the polaroid, is plotted together with the integrations giving piston speed and position. The open triangles are an attempt to read the velocity trace from the D/A converter from the polaroid. Integrals are for friction less motion for area under the breech pressure curve. The various firings showed a small fluctuation between this integration approach and the attempt to read position and velocity from the polaroid. For example, venting starts at 13.3 inch travel. The OBSERVED start on the scope occurs about 0.5 millisecond after the actual vent start since a release wave of about 3300 fps has to travel 20" back down to the pressure gage to be seen on the scope. The travel curve here is only about 11.5" whereas it should be about 13. This illustrates the unsatisfactory features of trying to extract too accurate numerical answers from this initial dynagun instrumentation.

A.4 Metallic Decelerator

In investigating a more economical piston decelerator, experimentation was initiated with type D metallic inversion (Reference 6) which employs a stainless, seamless tube, preformed at one end. The tube curls up on itself during compression with a forming die. A work-deformation system was desired to dissipate about 44,000 ft-lb of piston energy safely.

The 41, 42, 43rd dynagun firing investigated 16 gage SAE 1018 cold worked seamless tubing:

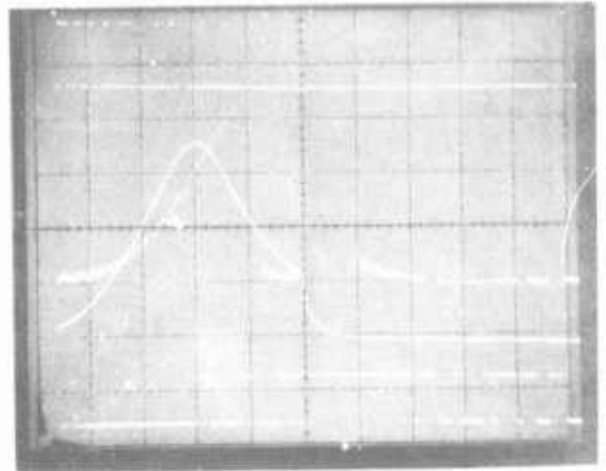
Firing 42, 43, Configuration:
(Die and tube are stationary with anvil.)



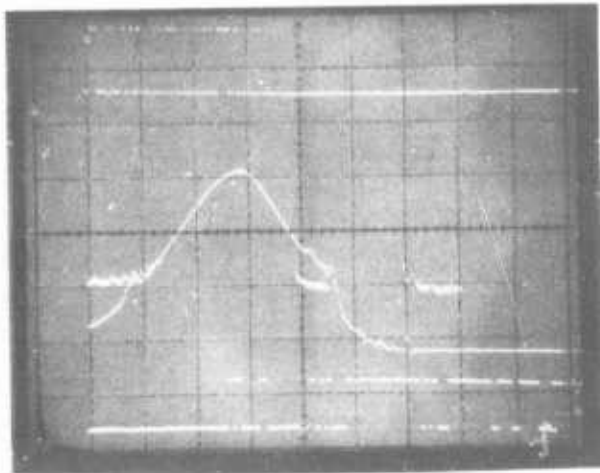
No. 25 LOT J

Figure 7. Dynagun P-W Polaroids.

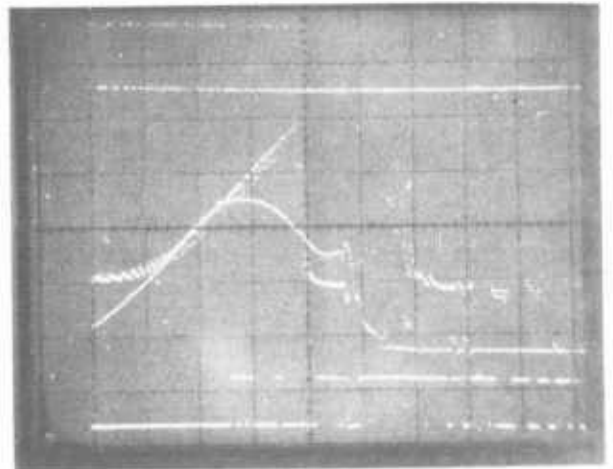
VERTICAL: 10 kpsi/cm
HORIZONTAL: 2 ms/cm
LOADING DENSITY:
67.5 g/131 cc = 0.515 g/cc



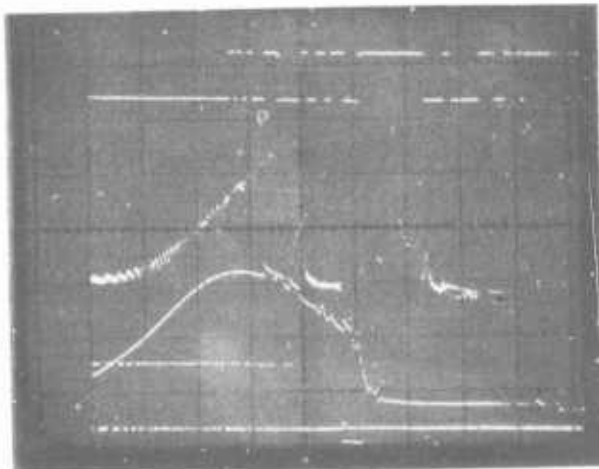
No. 31 LOT K



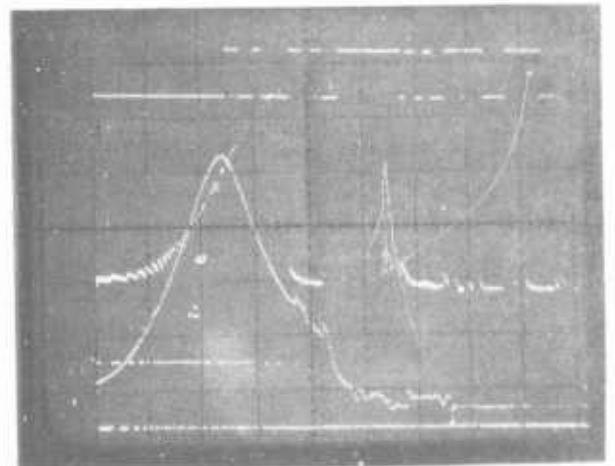
No. 32 LOT P



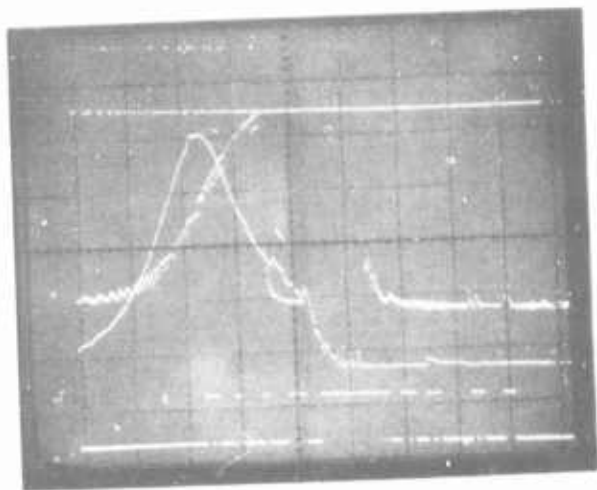
No. 33 LOT Q



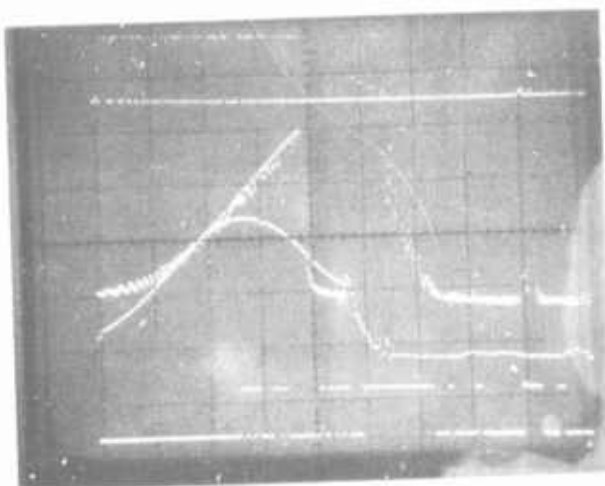
No. 34 LOT R



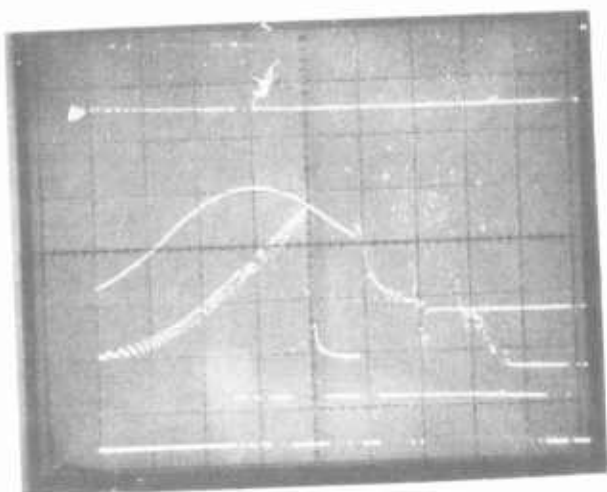
No. 35 LOT S



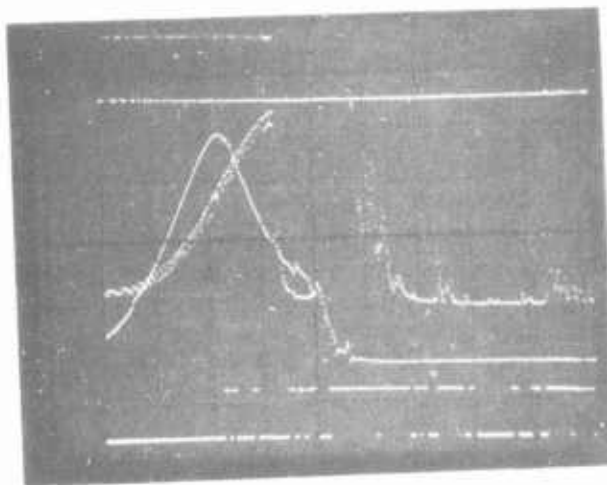
No. 36 LOT T



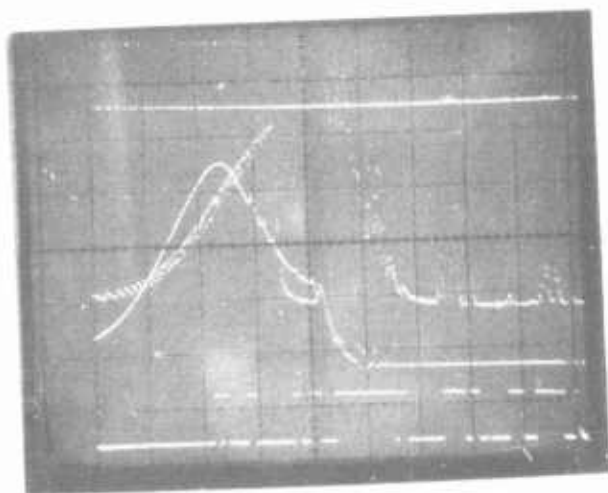
No. 38 LOT U



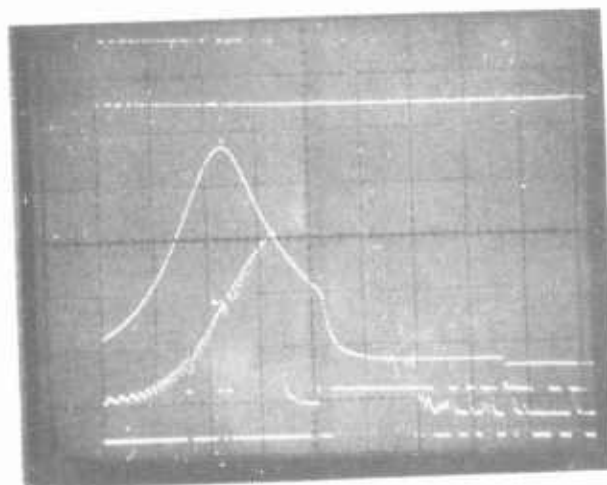
No. 39 LOT V

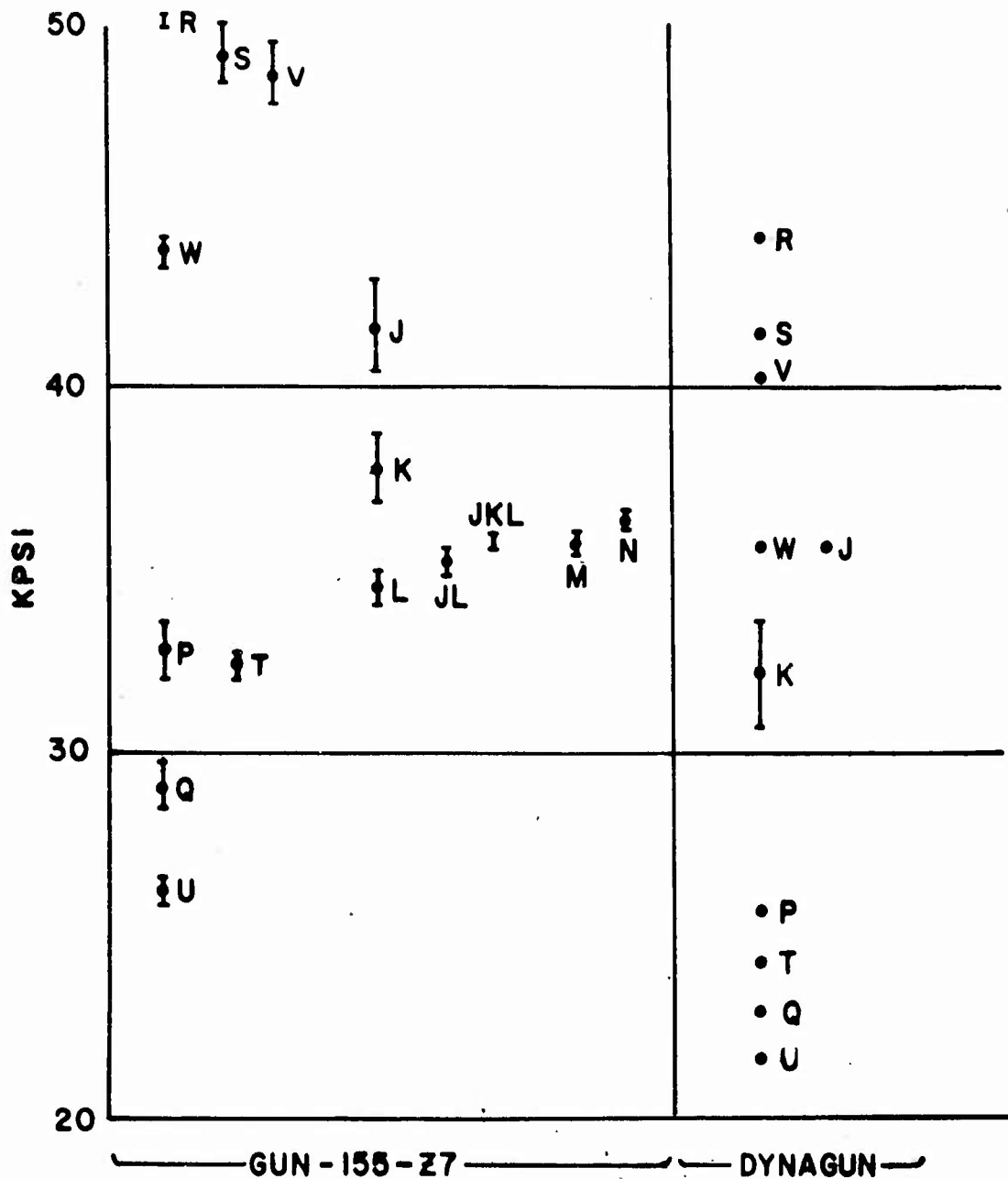


No. 40 LOT W



No. 47 LOT S





Length of bar for gun firings represents two standard deviations of 4 firings. Center represents the mean.

Four firings of lot K in dynagun.
 Dynagun loading density: $67.5\text{g}/8\text{ in}^3 = 0.515\text{ g/cm}^3$ 155mm zone 7, M126, M4A2 loading density: 0.462 g/cm^3

Figure 8 Gun and Dynagun Peak Breech Pressure

Table 3 Gun and Dynagun Pressure-Velocity ratios
Comparison of 155mm, M126 Howitzer and Dynagun Tests

Howitzer firings^a

Lot	Vel (fps)	Pk. Press (kpsi)	V_{max}/V_{max}^K	P_{max}/P_{max}^K
K	1848 ^b	36.09 ^b	1.0	1.0
R	1938	50.03	1.049	1.386
S	1930	49.43	1.044	1.370
V	1917	48.53	1.037	1.345
W	1883	43.67	1.019	1.210
P	1825	32.66	0.988	0.905
T	1805	32.25	0.977	0.894
Q	1773	28.99	0.959	0.803
U	1719	26.18	0.930	0.725

Dynagun Tests^c

K	272	31.3	1.0	1.0
R	290	43.4	1.066	1.387
S	280	41.1	1.029	1.313
V	280	39.4	1.029	1.259
W	268	35.3	0.985	1.128
P	254	25.5	0.934	0.815
T	254	23.8	0.934	0.760
Q	248	22.2	0.912	0.709
U	234	21.0	0.860	0.671

- a Represent average of four firings from each lot.
b This is the adjusted value to the reference fired for lots P-W.
c One firing of each lot. These velocities are calculated from the area under the pressure-time curve and are accurate to about $\pm 1.5\%$. They agree to about $\pm 3\%$ with the velocity primarily indicated by A-D converter from the magnetic sensor.

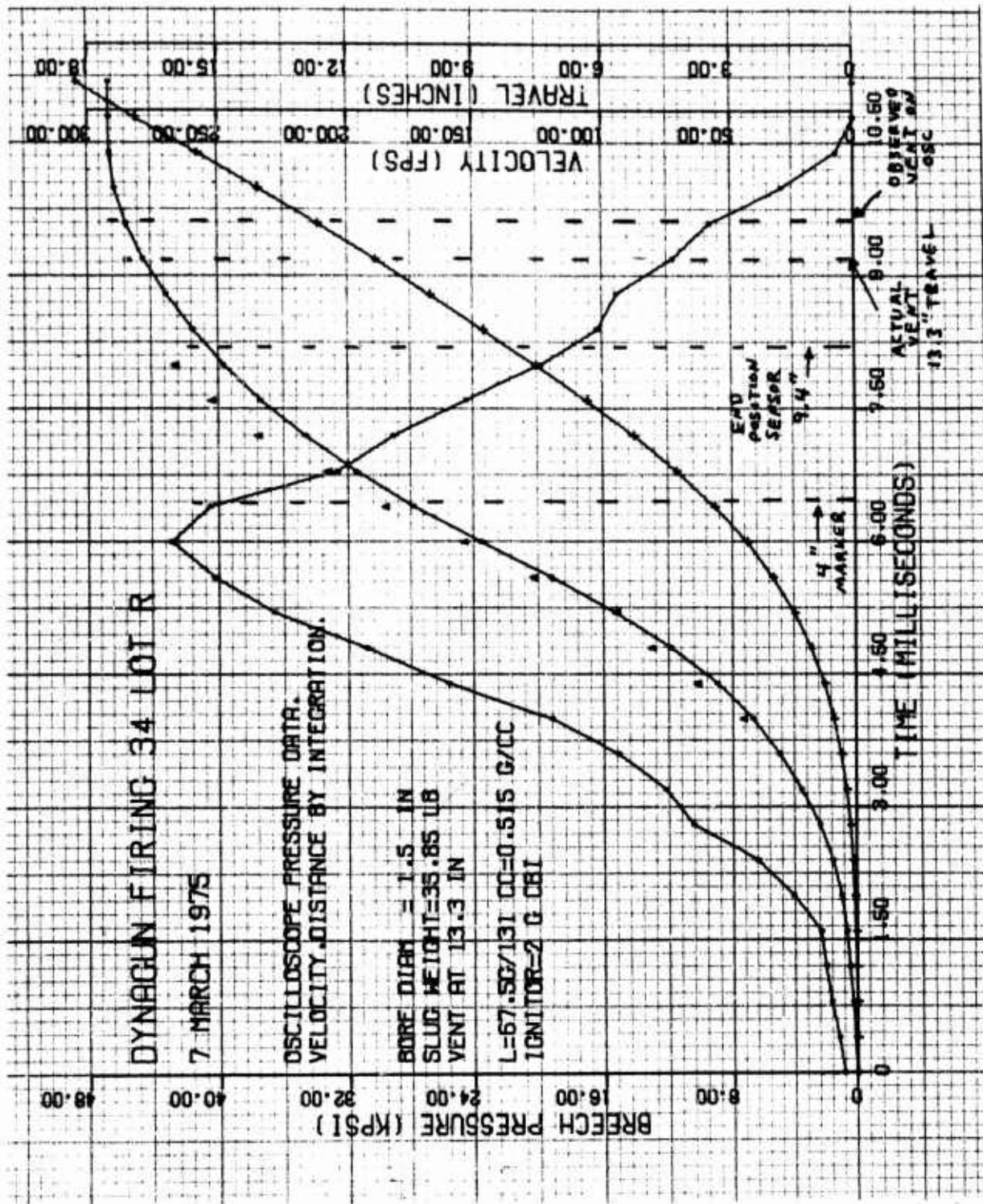


Figure 9. Dynagun Lot R Firing

In firing 41, however, the entire die, tube and anvil rode with the piston, increasing the piston weight by 9.2 lb. In run 43, a small bolt holding the piston's heat shield (1.5" diameter section) in front of the seal failed and the bolt was shaken loose. The piston struck it at the vent opening during rebound, and marred the piston finish. Some machining was required for the forward piston end, and together with striations caused by the initial blackpowder ignitor, the second series of lots P-W resulted in peak pressures consistently lower by about 2 kpsi.

In firing 43, for which the piston speed was increased from about 90 to 140 fps, the initial ripple which ordinarily extends for about 2 inches of tube length, became more pronounced before a final steady deformation condition showing absence of all ripple. This unfavorable aspect occurred since the die was forced to accelerate rapidly to match the piston's velocity. Further firings incorporated a die attached directly to the piston, with a stationary tube; and this removed the transient inertial gradients. This design removed all sign of unstable loading shown in these three tests. Also a solid backing for the anvil is needed to prevent eccentric or unstable loading and orientation of the tube during deceleration.

A heavier, 13 gage wall was eventually needed for higher velocities and several tests showed:

0.095" wall 3" O.D.

Average Deformation Force (lb):

[Static: 51,200
[Dynamic: 46,800 (170-270 fps)

The piston velocity increases about 9% during the acceleration from end of monitoring by the first position sensor to vent initiation. The entire $mv^2/2$ energy is dissipated into an average crush force F over distance x , and a small amount E for supporting dynagun stand motion or stress. For firing 68, with 13 gage wall, and 10.5" deformation and a speed of about 270 fps impact, the average calculated inversion load for the 36.2 lb piston is:

$$F(\text{lb}) = (mv^2/2 - E)/x$$

Neglect E : $F(\text{lb}) = 6.75 v^2(\text{fps})/x(\text{inch}) \approx 46,000 \text{ lb.}$

These calculated inversion loads are plotted in Figure 10. There were 19 successful firings out of 19 using this die-attached-to-piston design with 270 fps as the highest velocity attained.

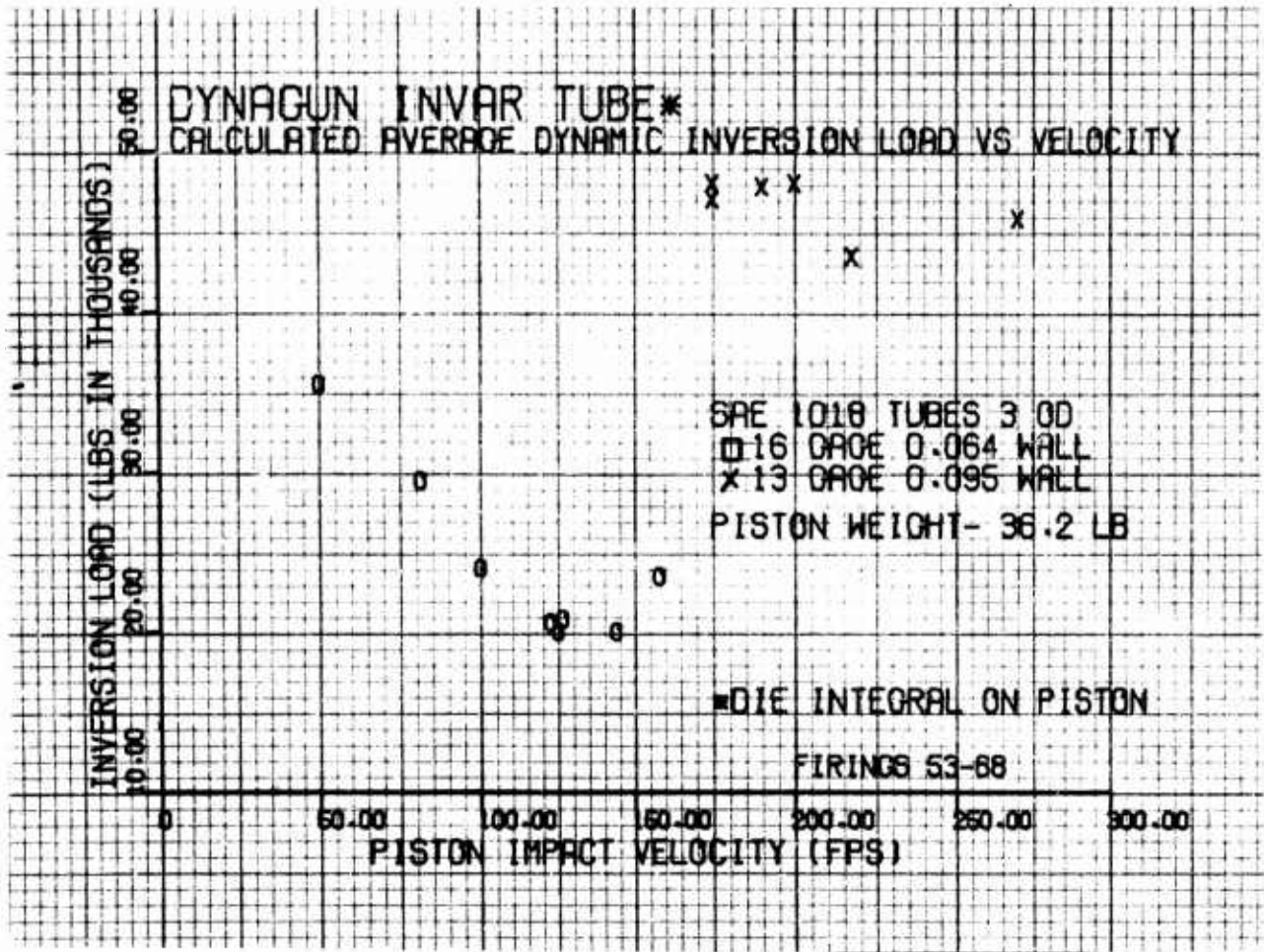
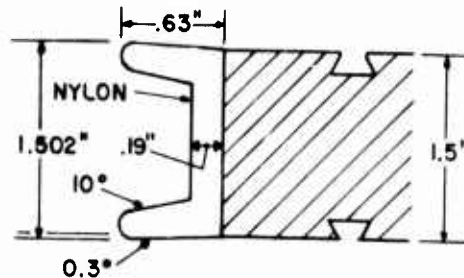


Figure 10. Invar Tube Inversion Load

A.5 Improvements

1. High pressure seal: The present configuration is made of nylon (6-10) of size:



Some improvement is needed, either a redesigned longer, two-seal piece (necessitates reposition of piston to keep same chamber volume), or employing an O ring in groove about the piston as a back-up seal as indicated in the sketch. Other designs suggest Makralon and annealed copper material (Reference 6).

2. The dynagun is being installed at Radford AAP for testing propellant production, with a redesigned piston and supporting stand, and relocated 2nd position sensor. To prevent or reduce piston rebound back into the combustion chamber, a vent in the closing flange now allows air escape to relieve the adiabatic compression spring. The dynagun will be rigidly mounted to a massive reinforced concrete block measuring 5x2x3 feet above the ground. This configuration does not allow recoil action to relieve rebound from stressed metal during the deceleration process.

Figure 11 is a diagram of the new four channel analog to digital-tape recorder system (4K, 10 bit words per channel with DC to 250 KHz (-3db) response per channel). Data can be digitized at a rate to 0.5 microseconds for as accurate as possible check on the mechanical performance of the entire system.

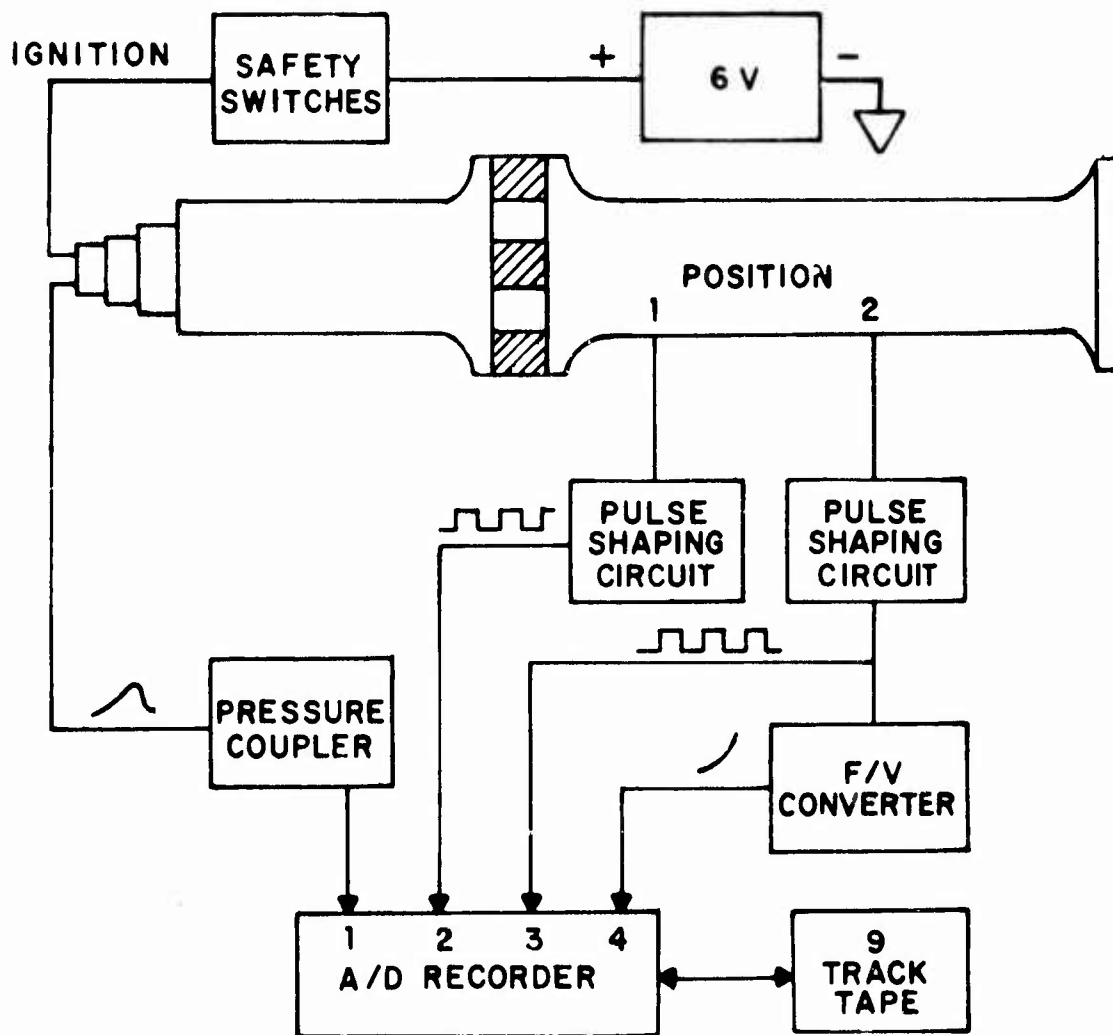
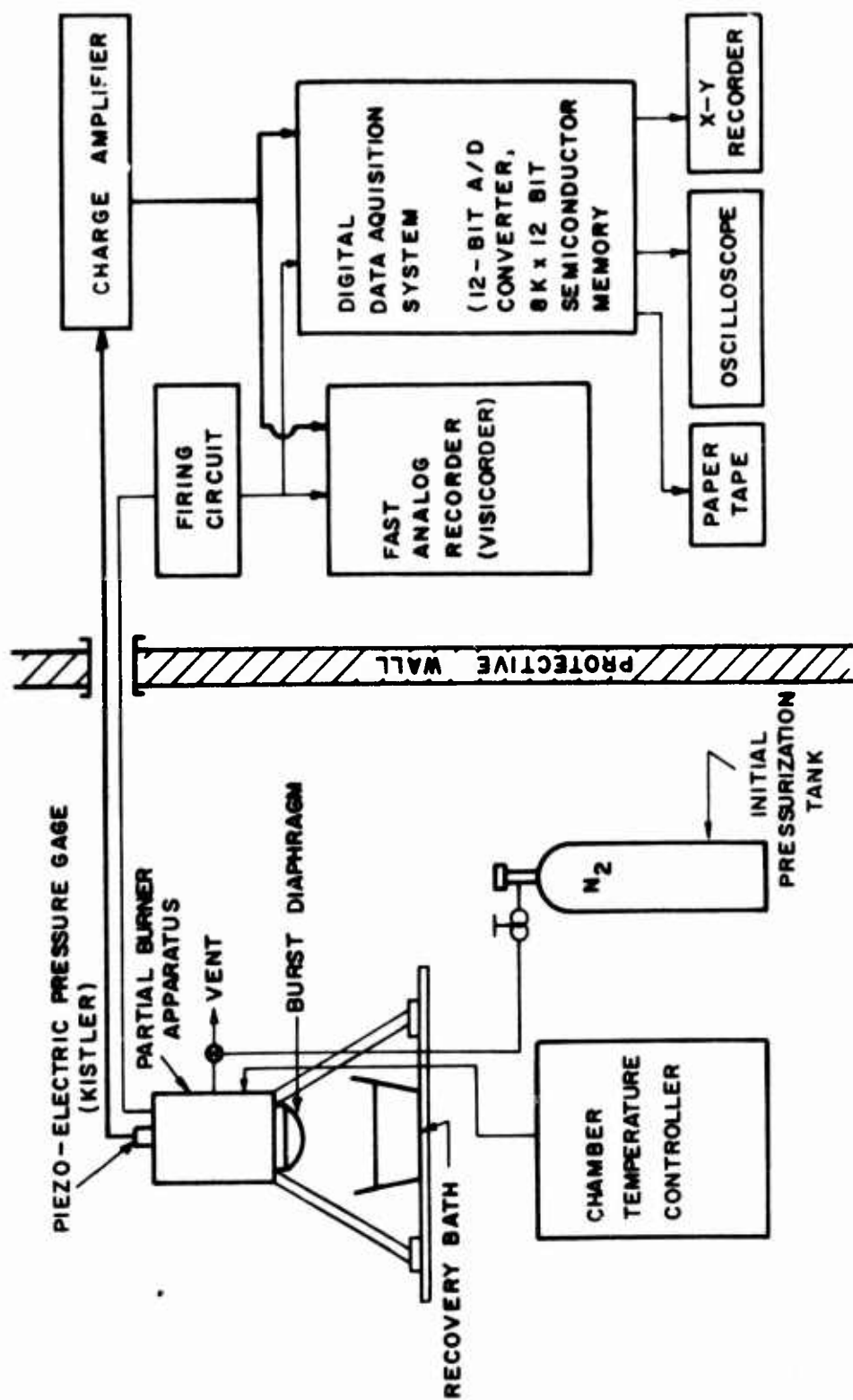


Figure 11 Dynagun Data Acquisition System

B. PARTIAL BURNER

Apparatus:

Further work was conducted at the University of Massachusetts on flame spread and ignition of single base propellant in a partial burner equipped with blow out disc, pressure transducer, and data acquisition system pictured in Figure 12. The burner was constructed out of a high pressure, large diameter, stainless steel check valve with the body altered to accommodate Fike Metals Corp. standard 2" rupture disc assembly. A series of aluminum inserts adapted the chamber to volume and shape for experiments. The burner is pictured on page 6.



SCHEMATIC OF THE EXPERIMENTAL APPARATUS

Figure 12. Partial Burner Instrumentation

Working pressure: 3000 psi
Volume: Variation from 42.5 to 473 cm³ (ALL EXPERIMENTS reported here closely simulated the dynagun chamber of about 1.5" diameter and 8.5 in³ (139cc).
Pressure gage: Kistler 603A

Tests:

For initial firings only 100, 10 bit records could be made. Initial pressure was always atmospheric, though it could be set up to 500 psi. The 2nd and 3rd firings had low loading density (0.2 g/cc) and soft ignition with an electrically heated wire around a grain in the middle of the propellant bed. Figure 13 is the pressure trace of the tests. Most of the grains were uniformly burnt. The lack of demarkation between burned and unburned surfaces was attributed to the long ignition delay allowing flame to cover the propellant before the pressure had a chance to increase appreciably. Test #2 with an 8% longer delay ended up with a faster pressure rise (probably resulting from propellant soak in the hot gases for a longer time, with this preheated surface yielding a faster flame spread rate).

Figure 14 plots dp/dt vs p for these firings. A linear plot indicates a pressure exponent of one, implying the pressure rise comes not only from the increased propellant burning rate, but a pressure dependent surface area growth.

With higher loading densities and CBI ignition, the CBI should increase the flame spread rate, but the higher densities produces faster pressurization so the flame spreading could become even more influential than at the lower, soft ignition, densities.

The fourth test used an electric match type M (ICI America Inc.) with 2 gram CBI assembly placed in the chamber opposite to the burst diaphragm which was located at the bottom of the propellant bed. At the higher densities, the pressure at burst was considerably greater than the static rated value. Also some propellant fractured on impact with the water recovery bucket. Burst pressure was 3400 psi.

Figure 15 shows the pressure trace with lot K, with the dashed line from data from an identical firing condition in dynagun firing #31. The ignition delay of 60 ms to reach 1000 psi is comparable to that reported for the dynagun.

Figure 16 is a dp/dt vs p plot for the pressure curve #4. Also plotted is the simple closed bomb chamber pressure rate equation where:

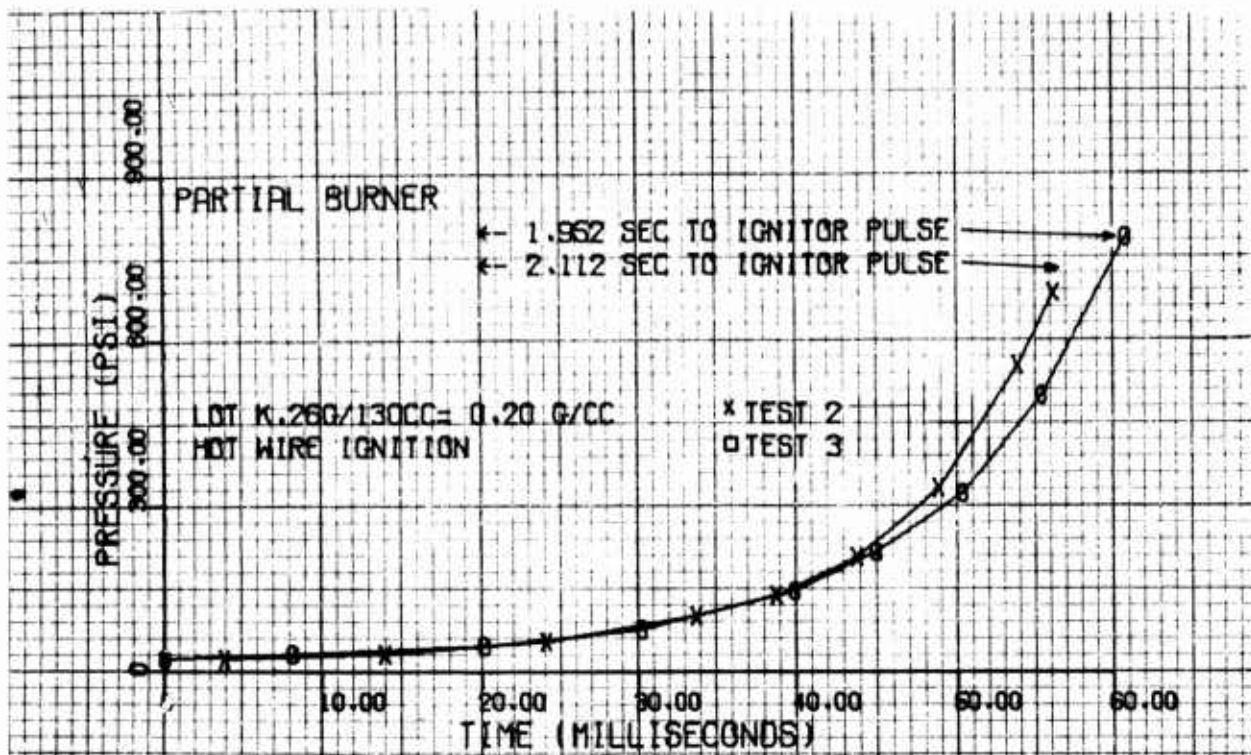


Figure 13. Low Pressure, Density Partial Burner Tests

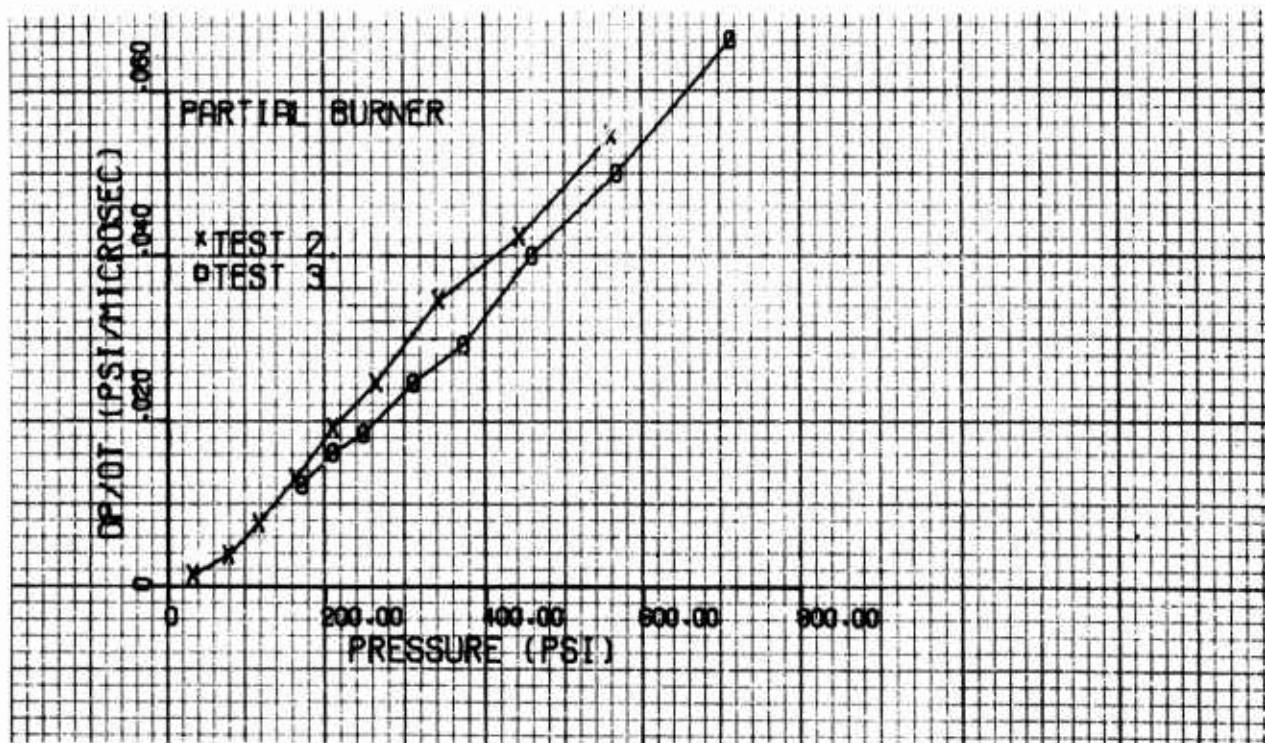


Figure 14. Closed Bomb Plotting of Burner Tests

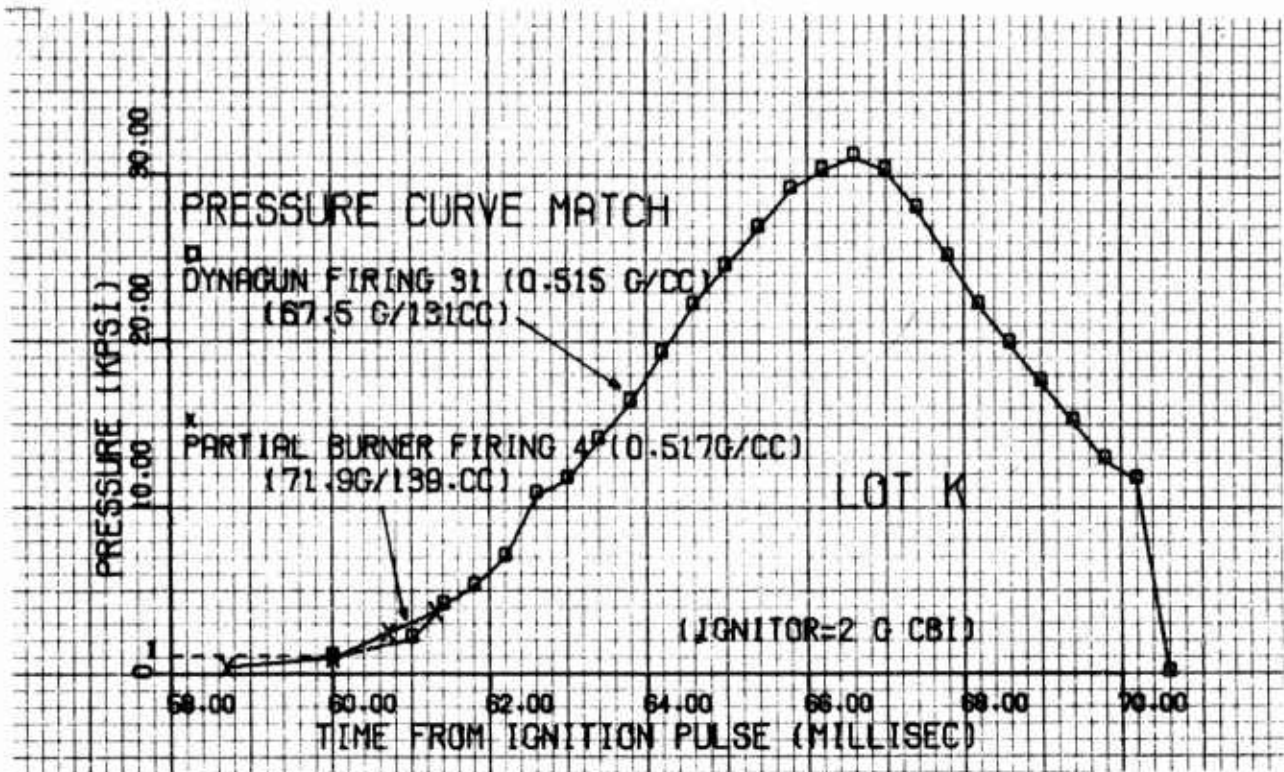


Figure 15. Partial Burner - Dynagun Pressure Match

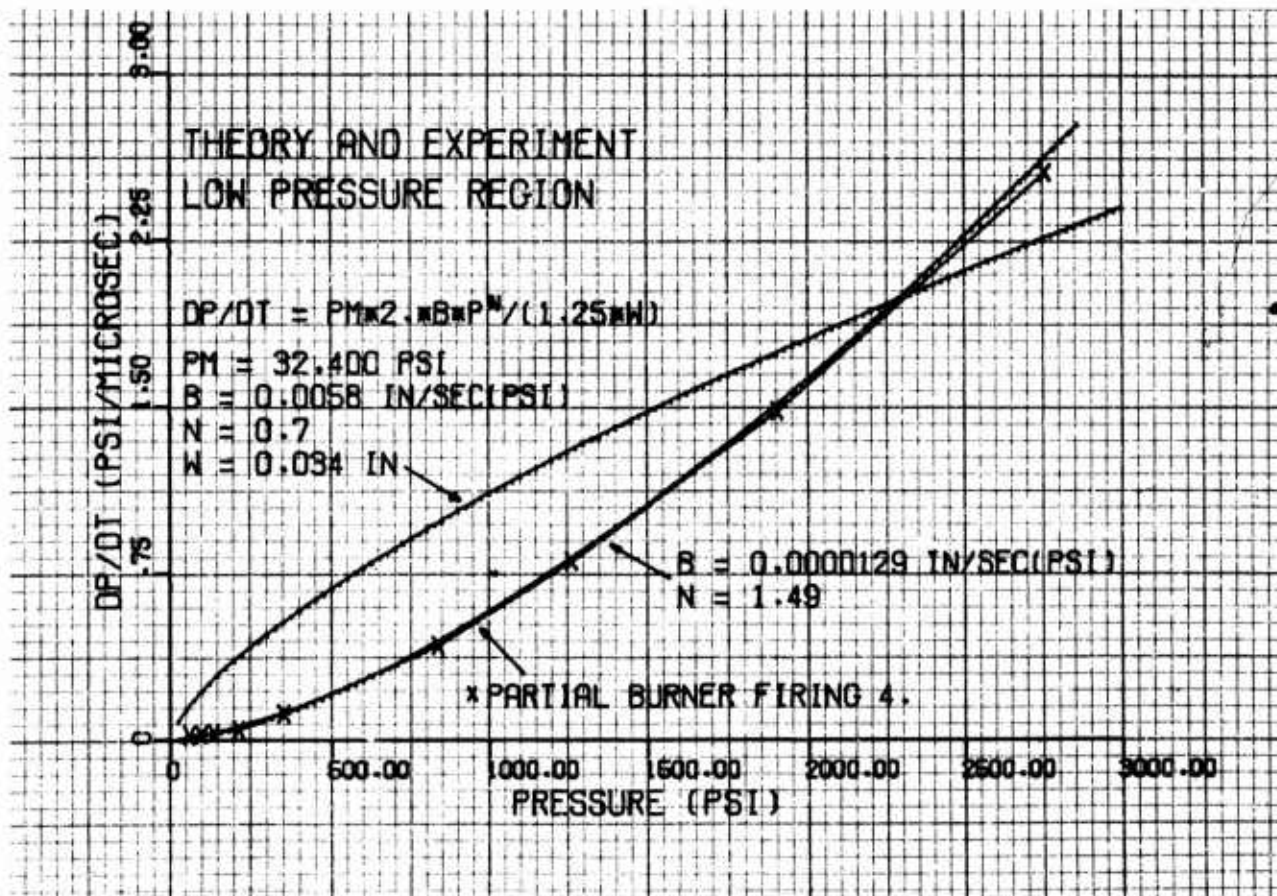


Figure 16. Closed Bomb Plotting at High Density

P_{max} - max pressure determined by loading density.
BPN - linear regression burn rate.
 $2/(1.25 w)$ is a form constant for 7 perf propellant.

Simple theory shows deceleration, whereas actual data accelerates up to 2000 psi. This behavior would imply that initially not all of the available surface was ignited, and the growth of burning surface area had a strong influence on dp/dt . A $\ln(dp/dt)$ vs $\ln(P)$ plot of test 4 gave a pressure exponent of 1.51, indicating pressure dependent burning surface area growth. At burst about 2% of the propellant had burned, and about 5% CBI remained in the chamber. All granules showed some burning activity on their entire exterior surfaces, though some appeared to have some portion of the surface unignited.

The ignition history of the perforations was more revealing since the perf diameters initially were uniform and could be measured accurately. Two histograms of the perforation diameters, from 140 randomly selected perforations for the unburned and for the burned propellant, gave:

Mean of perforations:	Unburned:	0.0144"
	Reported lot K:	0.0155
	Burned lot K:	0.0166

Histogram overlap implied about 14% of the perforations did not exhibit any growth up to 2000 psi. The conclusion is that flame spreading strongly influences the dp/dt in closed chamber combustion even at densities as high as 0.5 g/cm^3 , even with the use of energetic ignition such as an electric match with 2.8% CBI ignitor powder by weight.

Variable Ignitor; uniformity; ignition delay:

The next series of firings varied:

- a) Amount of CBI (none to 3 grams)
- b) Location of match-CBI assembly.

Figure 17 plots the p-t traces for seven conditions, all plotted to a 200 psi pressure point. The dp/dt vs p trace for these firings again shows that the weaker ignitions (except #5) show a more rapid pressure rate rise as 2000 psi is reached, than do the hard ignitions.

In search for a more consistent ignitor with less ignitor material, a spark plug type assembly was fixed in top of the burner: an ignition match was plugged into electrode holes, CBI poured into the small chamber, and the chamber sealed by two fine mesh stainless steel screens with four bolts. Figure 18 plots the uniformity test of this design with only 0.5 gram CBI. This design, from films of the ignitor operating at atmospheric pressure, indicates the screen

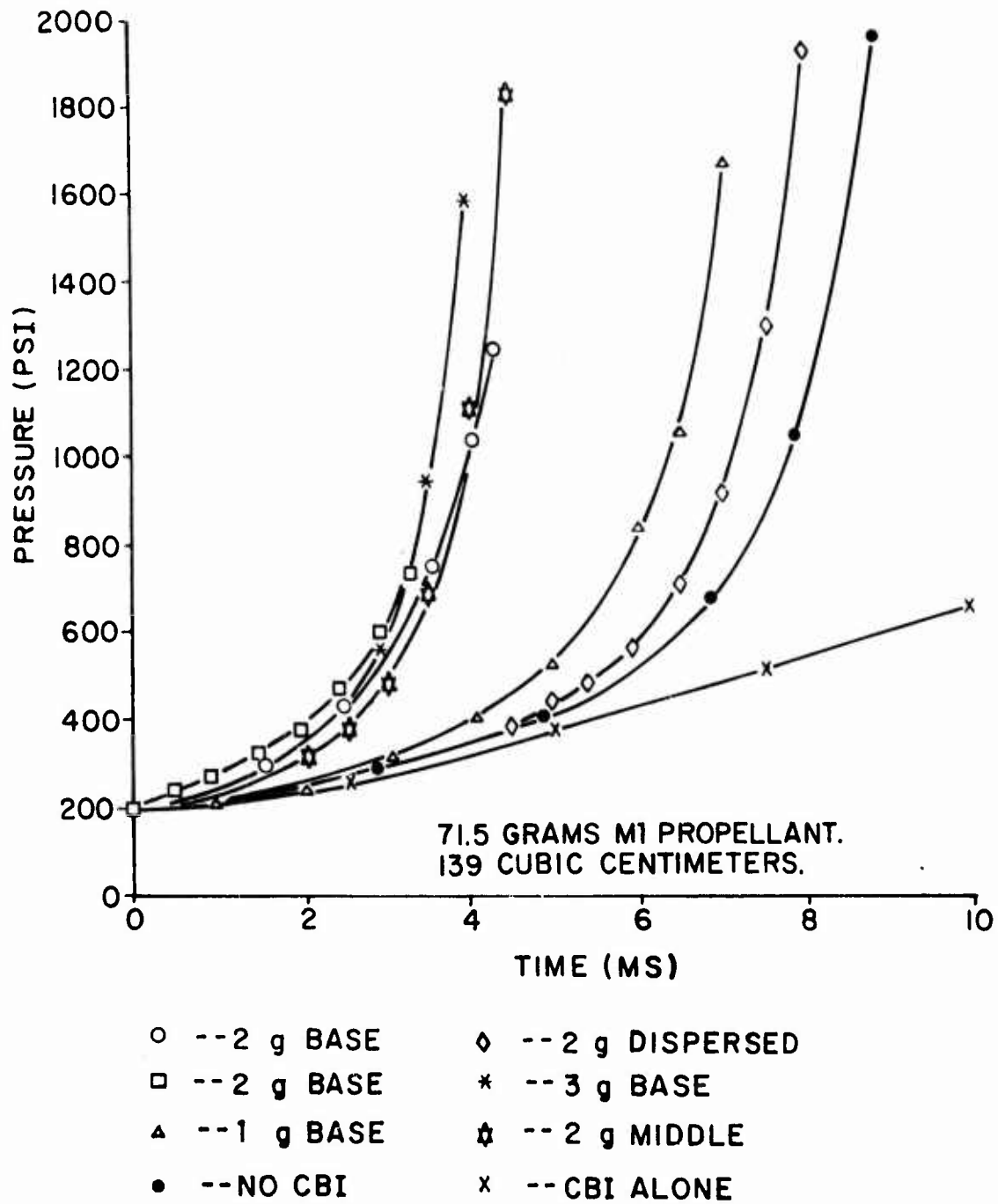


Figure 17. P-T for Ignitor Variation

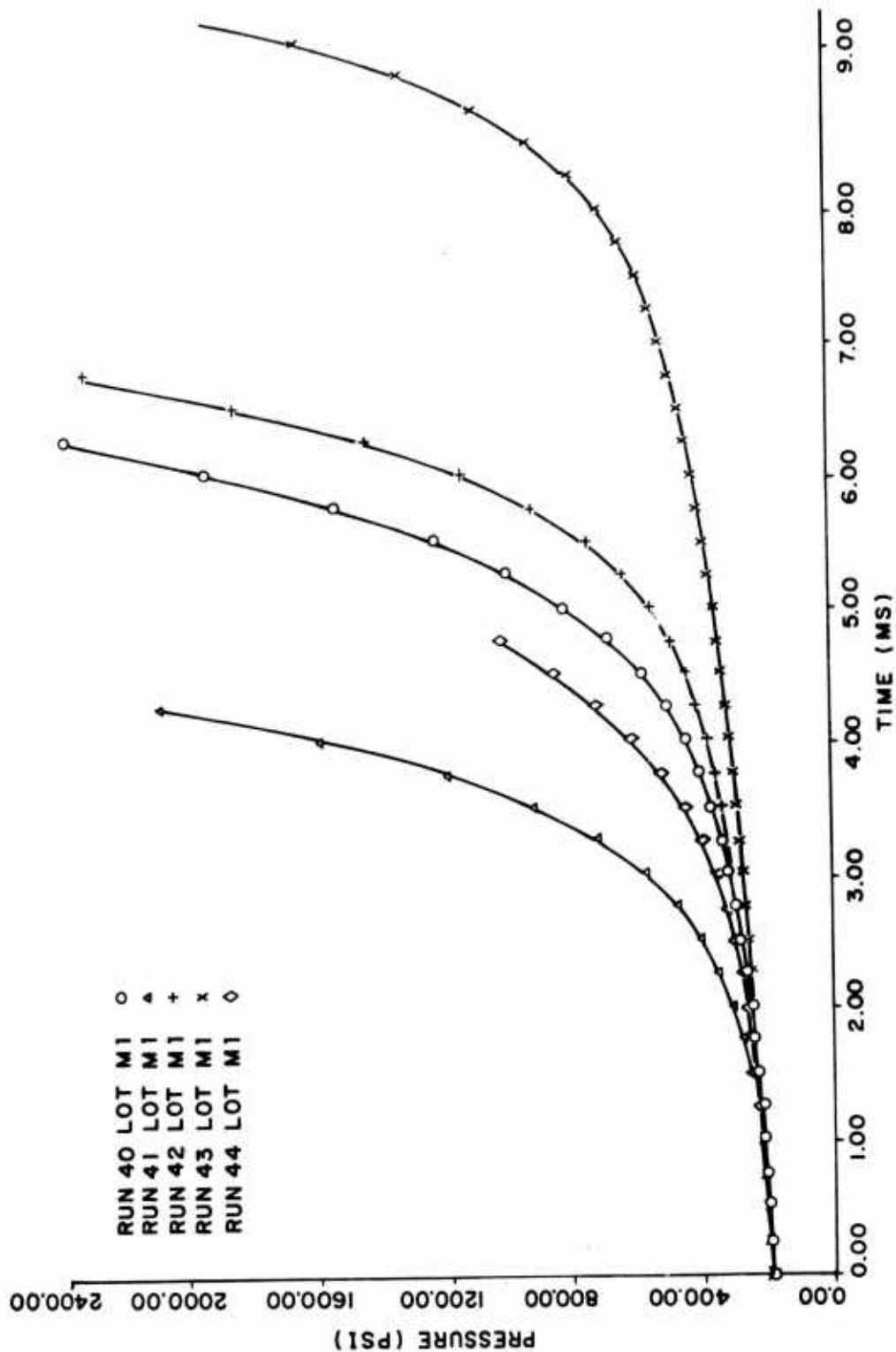


Figure 18. Burst Ignitor Uniformity

(Note: Ten burst ignitor firings of 0.5 grams of CBI with a match with mesh screens in a 130 cc chamber without propellant gave peak pressures from 130 to 210 psi with a rise time of about 12 psi/ms. A relatively constant 100 psi pressure persisted for a monitored interval of 100 ms after peak pressure.)

ruptures like a diaphragm, releasing a luminous column of flame. All are similar except #43 (the propellant was packed very densely) where the screen after experiment was observed not to have ruptured in a diaphragm manner.

This same ignition system using only 0.5 gram CBI and screen diaphragm was used on AUTOCAP lots, and the low pressure region is shown in Figure 19.

One conclusion is that the ignition delay (from fire signal to low pressurization) may indicate the nature of flame spreading in the propellant bed.

Some experimental efforts in varying closed bomb ignition have been reported:

(a) A 4.02% propane-95.98% air mixture at 60 psig, ignited by a small electrically heated single perf propellant grain, was employed in igniting single base, Reference 38250, M1 propellant for the 155mm howitzer, at 0.2 g/cm^3 in the 200 cc bomb. (M7 and ARP propellants in the "green" stage were also ignited with the same ease as dried samples). A parallel firing series was conducted with the nitrocotton-blankfire ignitor. Analysis of RQ indicated the propane-gas mixture gave significant decrease in variability of RQ and RF at the 0.75, 1 and 1.25 volt levels, but an unexplained large variation at the low pressure (8 kpsi) 0.5 volt level (Reference 7).

(b) Initial studies were conducted by confining the 0.2 g/cm^3 charge in a sealed cylinder containing a disc. A tissue-wrapped squib-blackpowder ignitor ignited single base AUTOCAP propellant lot K. For unconfined propellant, the mean time for burn from 200 to 2000 psi was 6.82 milliseconds. As the rupture pressure was increased from 125 to 330 psi, the burn time was shortened from 4.3 to 2.3 milliseconds (Reference 8).

C. HIGH PRESSURE ACOUSTIC BURNER

A compact high pressure burner has been constructed which burns propellant grains at a relatively constant pressure level up to 50,000 psi. High pressure is achieved by simple hydraulic water (or liquid) pressurization before grain ignition. Burning grains are found to emit high frequency sound in the 100 to 300 KHz range, which is detected by a piezo electric transducer attached to the outside of the steel cylinder. (The physical origin of this UHF sound is uncertain). Simultaneously a pressure gage monitors the relatively small liquid pressure rise during the burn. Only a very small free gas volume exists. The device is essentially a strand burner but with important differences: a) The only wire connection is an ignitor wire at the top of each

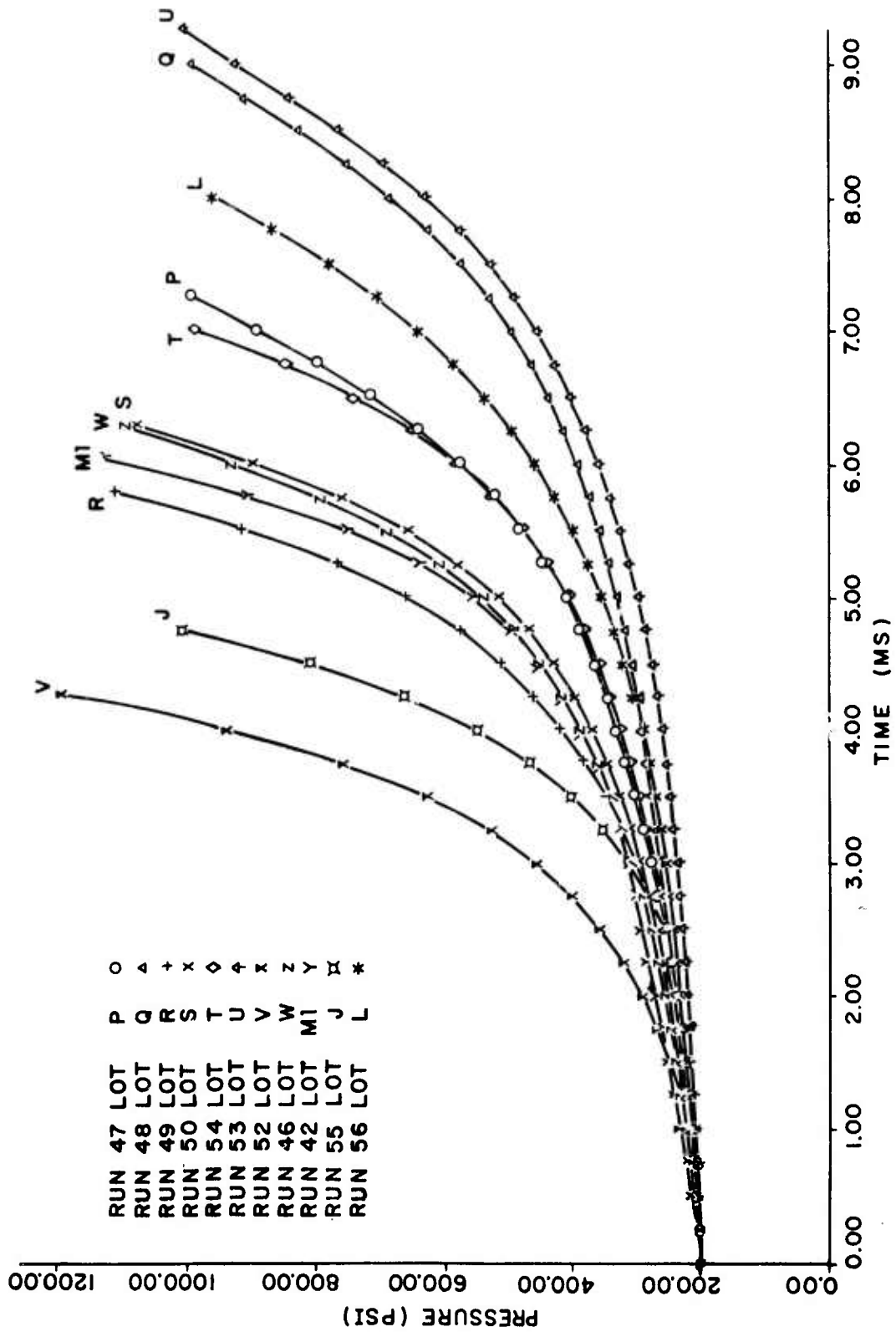


Figure 19. Burst Ignitor on AUTOCAP Lots

grain; b) a continuous time history of both sound emission and pressure rise is taken during the burn.

The phenomenon of UHF has been used to indicate the start and stop burn interval of rocket pressures (2 kpsi). Previous use of this technique at low pressures has been reported (Reference 9). Some past literature is only remotely related (Reference 10).

An intermediate low pressure (2 kpsi) combustor was first constructed from stainless steel and fitted with a hot gas jet, and an electric or percussion primer. After some exploratory experiments, the present high pressure burner was built early in 1974 under contract also with Princeton University (Guggenheim Laboratories), and tests were begun late in 1974.

The air-actuated hydraulic pump and part of the data acquisition system is shown in Figure 20. The combustor cell (burner) is behind the wall, and is sketched in Figure 21. A picture of the actual combustor and the tall pressure accumulator is shown in Figure 22. A special accumulator is not essential for the present combustor. As part of an effort to burn several grains in succession, Figure 23 shows a recent version of the ignition core with four separate grain holders. More are to be developed.



Figure 20 Acoustic Burner Pump

HIGH PRESSURE ACOUSTIC BURNER

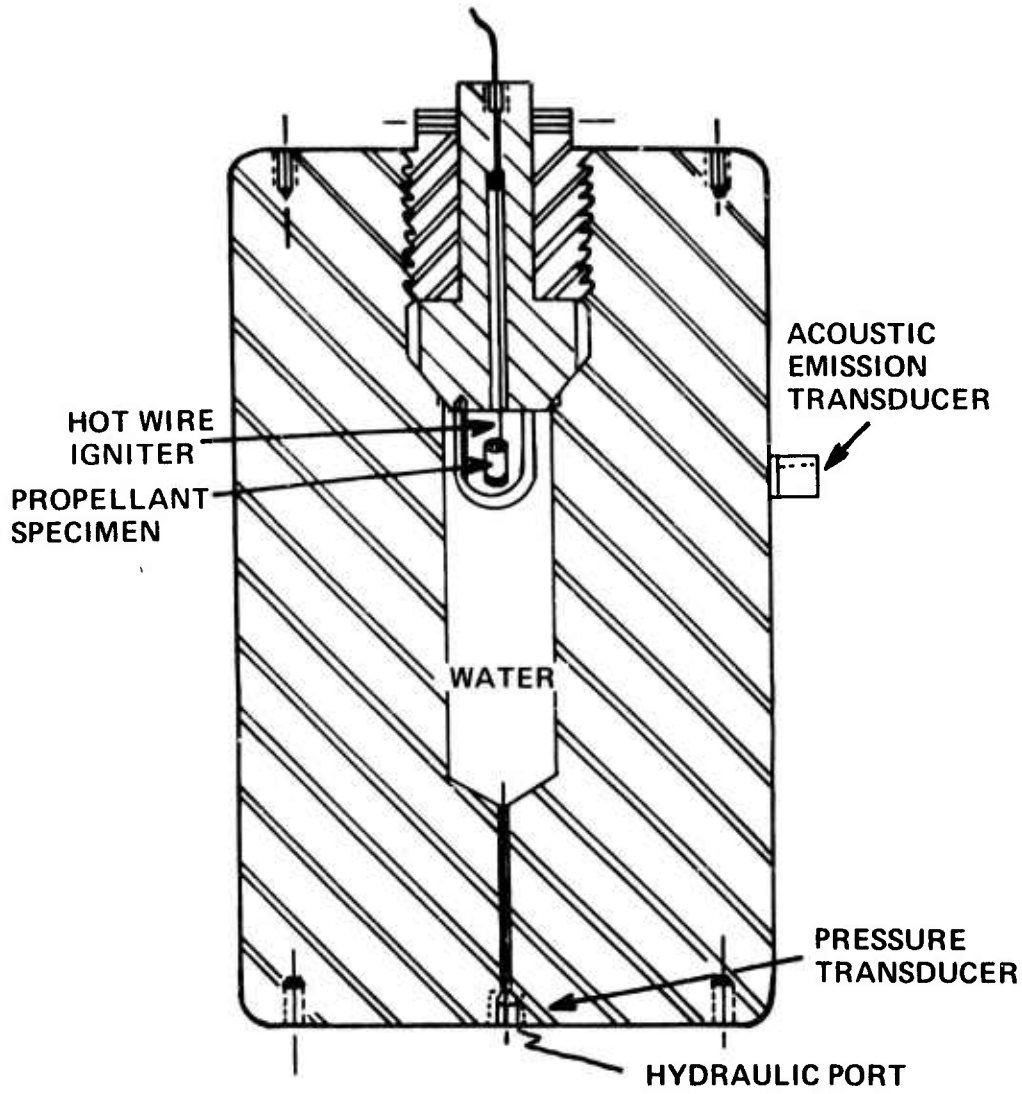


Figure 21. High Pressure Acoustic Burner

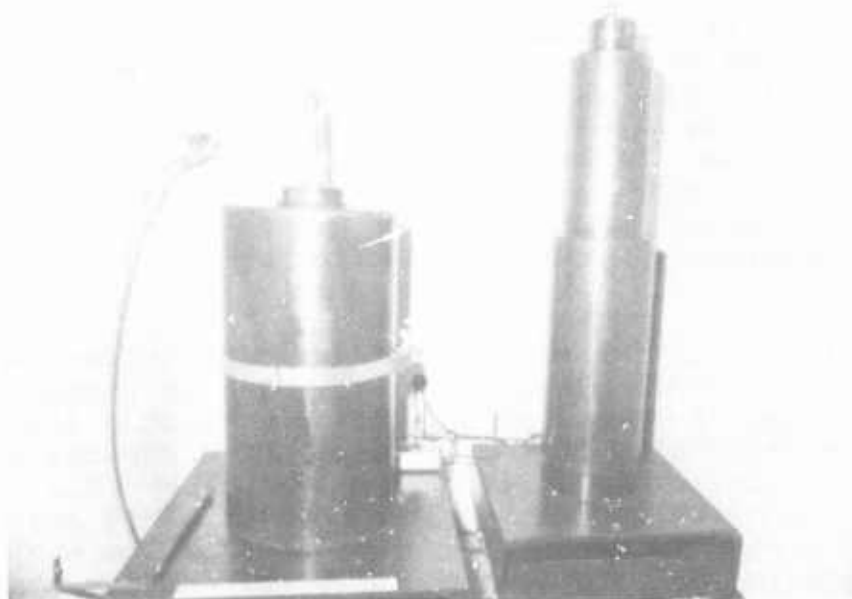


Figure 22. Combustor and Accumulator



Figure 23. Multi-Grain Ignition Core

The grain is cut to convenient length and a flattened, zig-zag nichrome wire is mounted with minimal cement on one end. The grain and a plastic base are installed in the combustor which is pre-filled with tap water of known temperature. The pump brings the system to the desired pressure in a few seconds, and (for uniformity) ignition occurs three minutes after immersion. The gas is in compression in a region immediately around the ignitor wire. (For single grain loading).

One of the initial methods for ignition to determine web action time (WAT) placed several grains in a graphite-lined crucible. A screen at the bottom prevented loss of grains into the fluid. A top orifice butted against an ignitor of nitrocellulose ignited with a nichrome coil. The combustor was prefilled with helium. In this WAT approach, the entire grains remained in a compressed helium environment. Emphasis was on obtaining rapid and uniform ignition over the grain ensemble.

A large number of tests were conducted to determine optimum ignition and suitability of grain inhibitor. Experiments have shown that the most reliable data results when single grains are burnt in candle fashion. When grains are burnt under liquid, the use of inhibitor appears unnecessary.

Single base M1 propellant lot U, both solid and perforated grains, was investigated extensively. The combustor has shown non-uniform burning that exists in these grains, and the variability is not experimental error. This was verified by strand burner tests and extinguished grain tests showing a concave rather than a flat burn surface. Non-uniform burning is detected by (1) gross noisy spikes in the acoustic signal, (2) a shortened over-all burn time, (3) minute discontinuities in the pressure trace, and (4) an obtuse pressure trace at the beginning and end of the burn.

The acoustic transducer output is filtered and frequencies above 100 KHz are amplified 60 db. The remaining signal goes through RMS conditioning for a convenient non-negative signal from a one to 10 volt level. Burn duration is the period of this signal. There is no monitored physical contact with the grain, except with the ignition wire touching the top of the grain. The signals are digitized onto an A/D recorder, displayed on a CRT monitor and 7504 Tektronix oscilloscope with a 7D15 time interval measurement preamplifier. Data is also recorded on a high-frequency response analog tape recorder.

One of the early traces is shown in Figure 24 for a two inch length of uninhibited solid strand from lot U at 20 kpsi

in 17.2°C water (Jan. 9, 1975). This is a rather uniform burn and time markers are 10 ms. The burn rate was 10.57 cm/sec. The four channels on the trace are:

- Channels:
 1) RMS of UHF signal
 2) UHF acoustic signal
 3) Pressure rise
 (about 400 psi)
 4) 10 ms marker
 (TIME GOES TO LEFT)

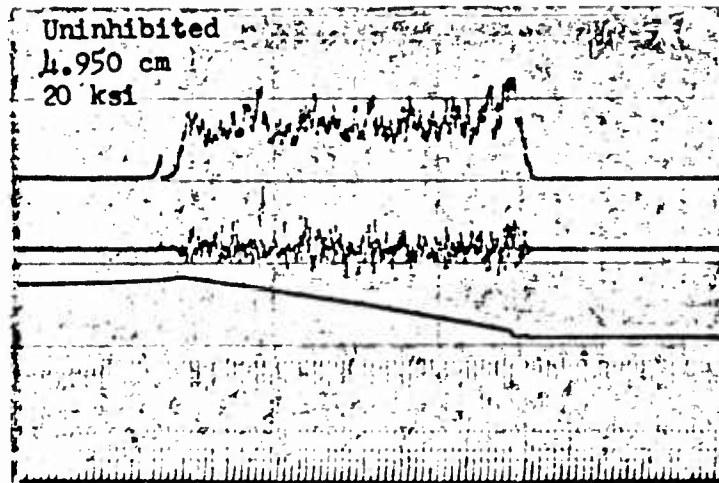


Figure 24. Acoustic Burner Trace

Data taken for lots U and P are listed in Table 4 with the initial mean pressure (individual pressures were measureable to 10 psi).

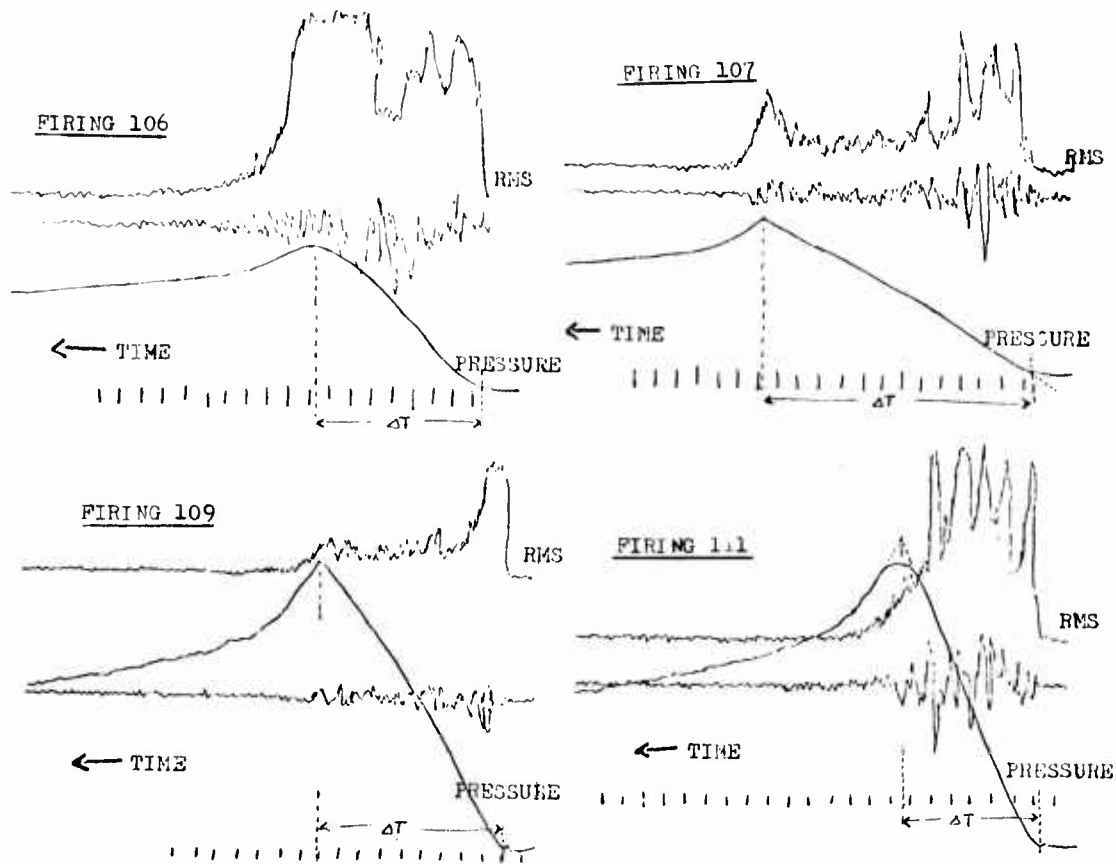
Table 4 Acoustic Burner Burn Rates

Pressure (kpsi)	10.21	20.17		30.17	40.18
Lot U (grains)	4.67	9.42	10.13*	12.96	17.34
	5.84*	8.80	9.18	13.07	17.67
	4.87	9.34	14.76*	14.78*	17.24
		9.31	9.05	18.07*	17.96
Lot P (grains)		10.17	11.78*		17.88
		11.17*	11.98*		17.70
		9.35	10.84		18.07
		13.26*	10.46		

* Acoustic emission irregular and obtuse peak pressure.

Four oscilloscope traces from lot U are reproduced in Figure 25 to illustrate the raw data. The more rapid burning grains in firings 106 and 111 illustrate the obtuse peak liquid pressure. Table 5 lists the coefficients B and n

Lot U firings: Oscilloscope traces of RMS UHF signal, the UHF signal, and water PRESSURE increase. These four pictures are taken from eleven made in a three hour period. Single grains were fired: Each $0.470 \pm .002$ " long. Ignition end was faced clean in a lathe. Grains were inhibited in perf holes and on outer surface with bituminous paint. Experiment done in water. Ignitor was 3.5 cm nichrome wire with 13 volts. 21.5°C water. 5/19/75/



Firing #	Pressure(kpsi)	ΔP (kpsi)	Burn time(ms)	Burn rate(cm/sec)
106	20	0.323	80.9	14.76
107	20	0.350	131.9	9.05
109	30	0.330	91.8	13.07
111	30	0.354	66.4	18.07

Figure 25. Selected Lot U Acoustic Burner Firings

when all reported 19 points for lot U were fitted to a power law, and for 14 points (with the five excessive burn points omitted). These coefficients were used to predict muzzle velocity and chamber pressure with an interior ballistic code employing also the Blake code. (The Blake code calculates several thermodynamic properties and gaseous products of solid propellant compositions as a function of pressure and temperature). Previously this ballistics code had been used to predict muzzle velocity and pressure in the J to W AUTOCAP lots (engraving profile kept same for all runs, etc.). Merely substituting B and n for lot U (no other changes) gave excessive muzzle velocity and pressure. The details and implications of this result have not been investigated.

Table 5 Ballistics Calculation for Lot U ^a

	B (cm/sec/psi ⁿ)	n	R ^e	Model Prediction	
				Velocity (fps)	Peak Pressure (kpsi)
CB ^b	0.01265	.639		1719	26
ABC	0.001036	.921	.9521	1849	42
AB ^d	0.000792	.943	.9987	1833	40

- a- For power law: $r(\text{cm/sec}) = B(\text{cm/sec/psi}^n)P(\text{psi})^n$, for zone 7, 155mm, M4A2 charge.
- b- B and n derived from Picatinny closed bomb data from 25 to 60% peak pressure.
- c- B and n from power fit for all 19 acoustic burner data.
- d- B and n from power fit to exact data from 14 acoustic burner data.
- e- Correlation coefficient of B and n fit to data.

The burning rate variation observed in lot U was further confirmed by burning solid strands in a 6 break wire chimney burner. Accuracies are generally better than 1% by this method; but the sample gave burn rate variations as high as 10%. The uneven burn might be attributed to incomplete mixing as globules of unmixed nitrocelluoues were found randomly located in cut-open grains. Grains of T, U, P, and Q lots were also x-rayed, but only obseravable on the negatives, were bright specks scattered rather uniformly through the grains. Lots T and U (higher K2S04 content) had higher density of these bright specks, possibly due to the greater absorp-tivity of potassium and sulphur to x-rays used.

Figure 26 is a tabulation of burn rate data for lots T, U, V, W. The strand and closed bomb data is from Picatinny Arsenal. For lot U, the mean of the acoustic burner closely follows the strand burner results. The actual acoustic

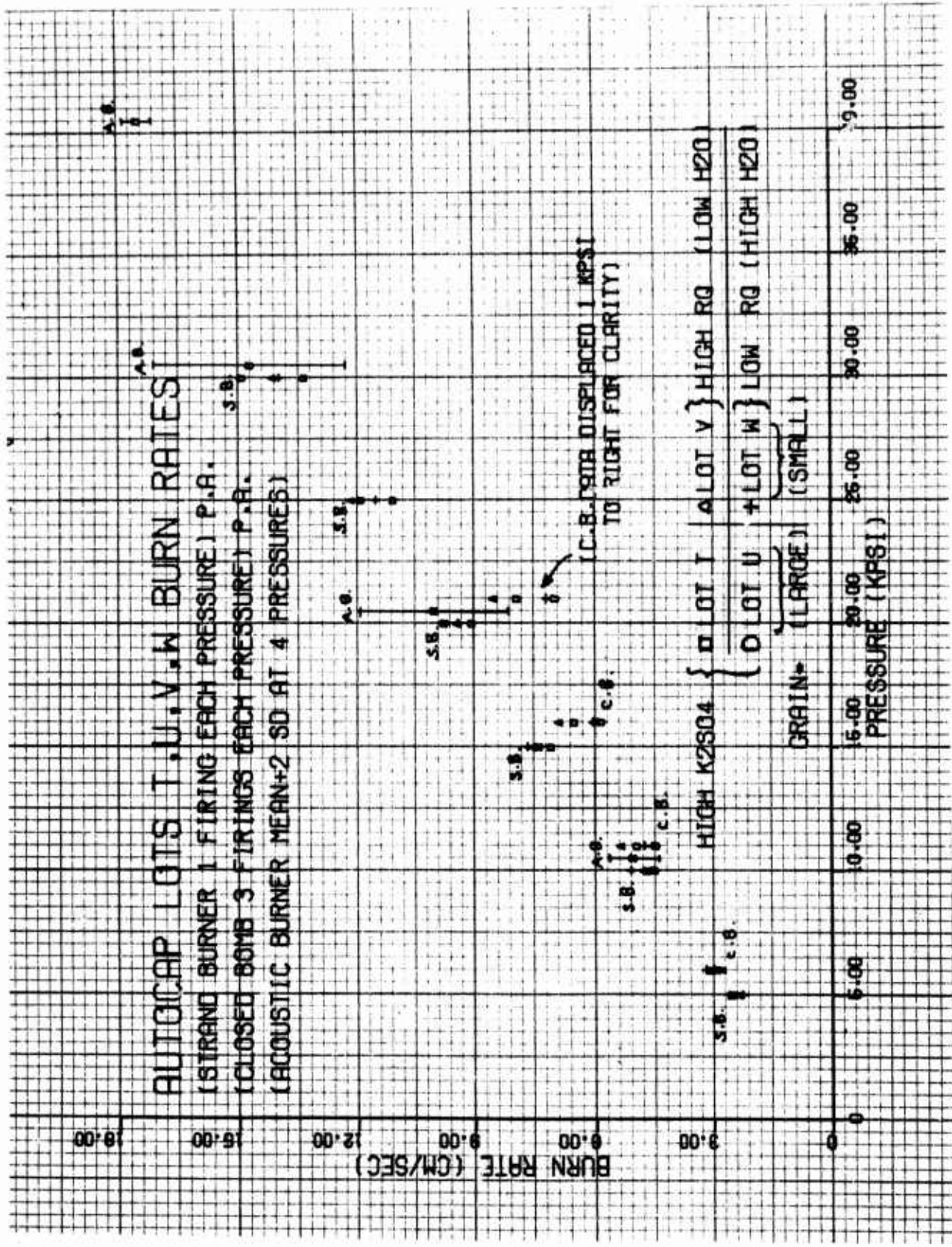


Figure 26. Burn Rate Plot Comparison

burner rates are not plotted, but only the mean with one standard deviation extending in either direction from the mean. The closed bomb derived burn rate (up to 20 kpsi) follows a lower slope.

Future Plans:

Though the device was originally intended to obtain direct burn rate measurements for use in interior ballistics codes for the AUTOCAP program for muzzle velocity and pressure prediction, it became apparent that the device had merit in quality assurance of propellant. The combustor is presently located at the Guggenheim Labs and further tests are planned with single and double base and solvent rich ("green") propellants.

An intended use is monitoring burning characteristics of solvent rich grains soon after the extrusion process early in the production cycle for detection of anomalous burning that might arise from incomplete blending, porosity, or general process non-uniformity. Also the center rod of the combustor is being redesigned to accommodate seven individual grains which will be ignited in succession to increase the number of grains tested per loading.

D. EGLIN SCALAR GUN

A previous report (Reference 1) described the Eglin scalar gun, a smooth bore artillery piece that fired expendable mild steel slugs for simulating 175mm gun firings with 6 off-spec lots of M6 produced early in the AUTOCAP program. Figure 27 is a picture of this gun and Figure 28 shows the case and slug components used in the 155mm firing simulations. The linear regression for the 175mm gun velocities and the scalar gun velocities for the M1 lots A through H (omit lot E) was found to be:

$$V(\text{fps})_{175\text{mm}} = 1915. + 0.396 V(\text{fps})_{\text{scalar}}$$

with a correlation coefficient only 0.920. Only one firing of each lot was done in the scalar gun.

Four carbon steel shear pins (about 1/8" diameter) held the slug to the adapter head for the 75mm brass case, and some additional shot start pressure was achieved by a small circumferential ridge near the base of the slug. A gas seal was provided as the flange was wiped away by the barrel bore.

However, at the termination of these M6 tests, examination of the gun revealed serious erosion at the breech end of the bore caused by the steel slug ridge used to produce obturation and partial shot start. For the M1 propellant firings for 155mm simulator, the tube was honed to 33mm diameter, with shot start provided by the 4 carbon steel pins alone (about 2500 psi), and the ridge was replaced by a groove with O-ring assembly for the gas seal. The gun and simulator parameters are listed in Table 6.



Figure 27 Eglin Scalar Gun for 175mm, 155mm firings

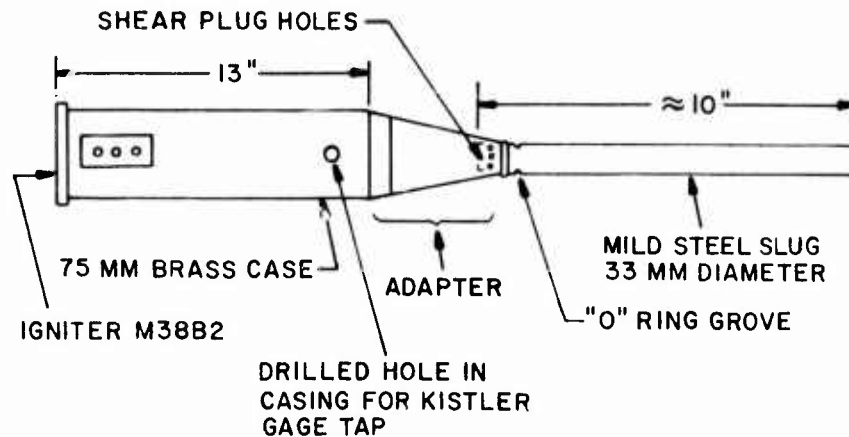


Figure 28 Case-Slug Assembly for Scalar Gun 155mm. M126 Firings

Table 6. Scalar Gun Parameters for 175mm, 155mm, M126

	175mm Simulator	155mm Simulator	155mm (M126) Howitzer
Slug weight w_s (lb)	3.56	3.77	95
Propellant weight w_p (lb)	2.27	1.19	13.15
Chamber volume (in^3)	96.5	96.5	805
Load density (g/cm^3)	0.651	0.341	0.457
Slug diameter (mm)	30.	33.	155
Slug travel (in)	120.	120.	116.
Shot start (psi)	6000.	2500.	4000.
Ref Speed (fps)	2740.	2067.	1850.
R ratio $(v_{co}/V_{co})(D_s/d_s)^2$	1.22	2.643	--

The firing results for the scalar gun, 155mm simulation are in Table 7.

Table 7. Scalar Gun Simulation of 155mm, M126

Propellant Lot	Velocity(fps) (mean)	Peak pressure(kpsi) (mean)
M1 ^a	2048,2055,2096	2067
Q	1850,1848	34.5,35.5,37
R	2120,2115	23,23
T	1913,1900	40,40
V	2076,2084	2118
W	2035,2051	1907
M1 ^a		2080
S ^b	2172,2176	37,37.5
		34.5,34.5
		2043
		2047
		38
		49

a Lot number unknown.

b Slug weight for S was increased to 1750 grams (3.858 lb) to lower muzzle velocity.

The actual scalar gun and 155mm howitzer velocities are plotted in Figure 29 with the linear regression equation and the rather high correlation coefficient. The fit does not include the lot S. Since a higher slug weight was used for lot S, the approximation that velocity varies inversely as the cube root of the slug weight estimates that the velocity would have been increased 0.77% to 2191 fps if the same slug weight had been used as for the other lots. This brings lot S firing even further from the regression line. Furthermore, the reference firing with lot S was 20 fps lower, yet 2 kpsi higher in peak pressure when compared to the mean reference data with the other lots. Also the first three reference firings have wide scatter in velocity. These factors prevent an estimate of what would have been the ranking of lot S, which has shown an anomalous behavior.

The comparison of the pressure differential and velocity differential between reference propellant and AUTOCAP lot firings in the 155mm howitzer (and also in the scalar gun) show that lots QRTV show variations in the same direction in the test device as in the actual howitzer. (Lot W showed positive differentials for the 155mm results, and negative ones for the scalar gun. Since the chamber volume was originally designed for the 175mm simulation, slug mass was increased for lot S to give the differentials:

Howitzer, Scalar Gun Differentials for Lot S:

Propellant	155mm Howitzer			Scalar Gun	
	Velocity	P. Pressure		Velocity	P. Pressure
S	1930	49.4	S	2174	49.
Ref	1855	36.7	Ref		
(68308)			M1	2047	38
S-Ref	= 75	12.7	S-Ref=127		11

The pressure differential is very similar, but the similitude is not exact and dictates experiments with a smaller chamber volume and heavier slug.

Figure 30 is a plot of the chamber pressure for lot S (one of two from scalar gun) and one of the four fired at zone 7, 155mm, M126 at Aberdeen. The simulator curve is still broad based. A good match between velocity (2174) and barrel travel (120") was obtained by using:

$$P_{base} = P_{chamber} / (1 + (w_p Z / w_s))$$

where Z is a linear ramp to one over the pressure range from zero to slightly past peak pressure. The base/chamber pressure ratio for the expansion part of the pressure curve was about 76%.

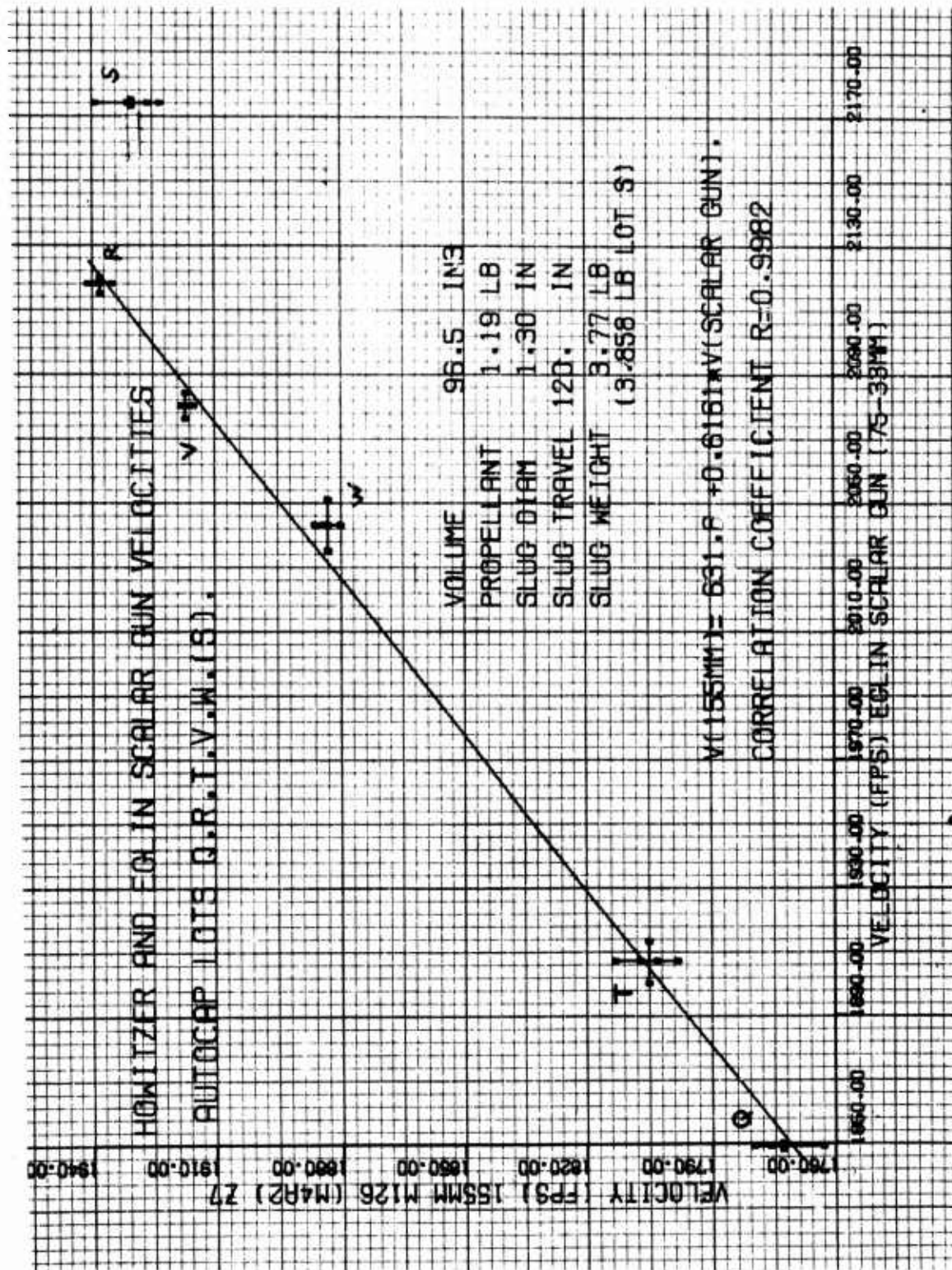


Figure 29. Scalar Gun 155mm Simulator Plot

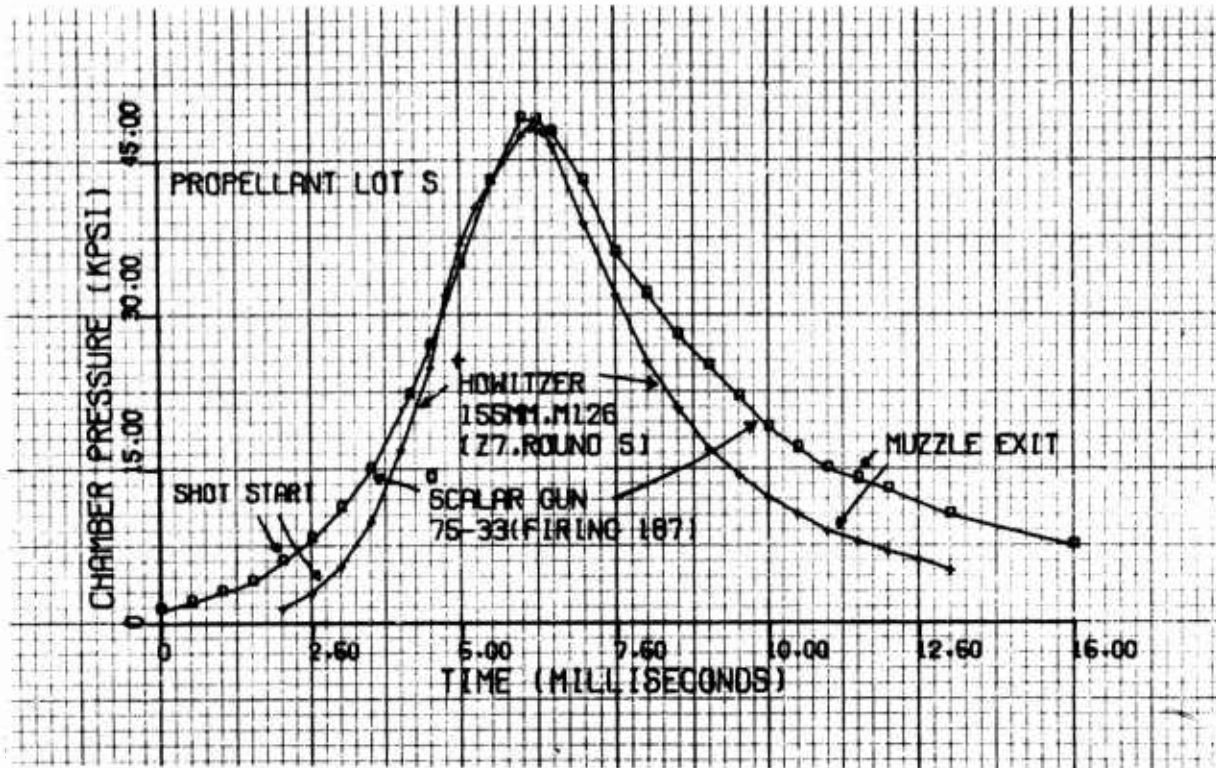


Figure 30. Pressure-time for Lot S.

CONCLUSIONS AND RECOMMENDATIONS

1. The second phase of the dynagun firings (~~initiating in August 1976~~) with the improved data acquisition system, should lead to a more quantitative judgment on the dynagun reproducibility, reliability, maintainability, and ballistic correlation. In an uncertain state is the reliability of the present high pressure seal, which may eventually need some redesign, and the impact of the high heat loss.

2. The present two grams of CBI with bagged match ignitor system for the dynagun is tolerable. The employment of a rapid-pressurization, lower ignitor load assembly would require machine redesign of the dynagun breech, and its recommendation is uncertain at this time.

3. A more extensive series of tests with various kinds of propellant is recommended for the high pressure acoustic burner to acquire a basis for judgment on its applicability to burn rate measurement and quality in-process propellant control. This is being addressed in a present program.

4. The limited number of scalar gun firings prevents clear judgment on this system. The data shows favorable results and the device remains a candidate for propellant ballistic acceptance.

REFERENCES

1. Domen, J., Feasibility of Scaled Down Guns to Duplicate Large Caliber Interior Ballistics, Report No. ASRSD-QA-A-P-64, July 1974; Picatinny Arsenal.
2. Domen, J., Interim Report on Modernization of Closed Bomb Testing for Acceptance of Single Base Propellant, Report No. QA-X-016, May 1976, Picatinny Arsenal.
3. Krier, H., and Black, J., The Concept and Design of the Dynagun Ballistic Simulator, U. of Illinois Technical Report AAE 74-7, Dec. 1974.
4. Krier, H., Neitzke, T., Adams, M., Black, J., Meister, E., Solid Propellant Burning Evaluation with the Dynagun Ballistic Simulator, U. of Illinois Technical Report AAE 75-8, July 1975.
5. Serao, P., A Mathematical Prediction of Ballistic Performance for M6MP Propellant in the 175mm Gun System, Report No. ASRSD-QA-A-P-58, April 1974, Picatinny Arsenal.
6. Moreau, R., Final Report: Task Order #74-99, #75-161, prepared for F.J. Fitzsimmons, SARPA-QA-A-P, Picatinny Arsenal, Sept. 1974.
7. Carter, H., Improving Precision of CB Testing by Substitution of Propane-Air Primer for Nitrocotton-Blankfire System, QA Investigation 483-A, Radford Arsenal, Hercules Powder Co., Jan. 1957.
8. Shulman, L., Comparative Burning Rates Analysis, in BRL RN 1883, 1975 Annual Review of ARMCOM Program, Fundamentals of Ignition and Combustion, May 1976, (Propellants Division, Picatinny Arsenal).
9. Koury, J., Solid Strand Burn Rate Technique for Predicting Fullscale Motor Performance, AFRPL-TR-73-49, Oct. 1973 (Air Force Rocket Propulsion Laboratory, Edwards, Calif).
10. Osborne, M., and Holland, F., Acoustical Concomitants of Cavitation and Boiling, JASA, 19,1 (Jan. 1947) pp. 13-32.

DISTRIBUTION LIST

	<u>Copy Number</u>
Commander US Army Armament Command ATTN: DRSAR-SC DRSAR-QAR DRSAR-PPI Rock Island, IL 61201	1 2 - 3 4 - 5
Office of the Project Manager for Munitions Production Base Modernization & Expansion US Army Development and Readiness Command ATTN: DRCPM-PBM-T Dover, NJ 07801	6 - 7
Office of the Project Manager for Cannon Artillery Weapon Systems US Army Development and Readiness Command ATTN: DRCPM-CAWS Rock Island, IL 61201	8 - 9
Commander US Army Development and Readiness Command ATTN: DRCRD 5001 Eisenhower Avenue Alexandria, VA 22304	10
US Army Research Office ATTN: Librarian Box CM, Duke Station Durham, NC 27706	11
Commander US Army Test and Evaluation Command ATTN: AMSTE-BB Aberdeen, Maryland 21005	12
Commander Aberdeen Proving Ground ATTN: STEAP-DS-TA STEAP-TL Aberdeen, MD 21005	13 14
Commander Army Ballistic Research Laboratories ATTN: AMXBR-IB (Dr. Ingo May) AMXBR-1, (Librarian) Aberdeen Proving Ground, MD 21005	15 - 17 18

DISTRIBUTION LIST (CONT'D)

	<u>Copy Number</u>
Commander Picatinny Arsenal ATTN: Technical Director	19
SARPA-QA	20
SARPA-QA-A-P	21
SARPA-QA-X	22 - 47
SARPA-FR-G-B	48
SARPA-FR-G-C	49
SARPA-FR-G-F	50
SARPA-AD-D	51 - 53
SARPA-AD-E	54 - 56
SARPA-TS-S	57 - 61
Dover, NJ 07801	
 Air Force Armament Laboratory ATTN: O. Heiney Eglin Air Force Base Eglin, FL 32542	 62 - 63
 Commander Radford Army Ammunition Plant ATTN: SARRA-QA Radford, VA 24141	 64 - 68
 Commander Frankford Arsenal ATTN: Librarian Philadelphia, PA 19137	 69
 Commander Indiana Army Ammunition Plant ATTN: SARIN-QA Charlestown, IN 47111	 70 - 71
 Commander Badger Army Ammunition Plant ATTN: SARBA-QA Baraboo, WI 53813	 72 - 73
 Commander Naval Weapons Center ATTN: R. Derr China Lake, CA 93555	 74
 Commander Watervliet Arsenal ATTN: Librarian Watervliet, NY 12189	 75

DISTRIBUTION LIST (CONT'D)

	<u>Copy Number</u>
Defense Documentation Center Cameron Station Alexandria, VA 22314	76 - 87
Naval Ordnance Station ATTN: 5232, A. Horst Indian Head, MD 20640	88 - 89
Naval Weapons Laboratory ATTN: Dr. J. East Dahlgren, VA 22448	90 - 91
University of Illinois AAE Department ATTN: Dr. H. Krier 101 Transportation Building Urbana, IL 61801	92 - 93
University of Massachusetts Mechanical Engineering Department ATTN: Dr. K. Jakus Amherst, MA 01002	94 - 95
Guggenheim Laboratories Princeton University ATTN: Dr. L. Caveny Princeton, NJ 08540	96 - 97
CALSPAN Incorporated ATTN: E. Fisher 4455 Genesee Street Buffalo, NY 14221	98 - 99
Pennsylvania State University Mechanical Engineering Department ATTN: Dr. K. Kuo University Park, PA 16802	100